arXiv:hep-ph/0608290v2 2 Dec 2007

Non-Perturbative Study of the Light Pseudoscalar Masses in Chiral Dynamics

José A. Oller[#1] and Luis Roca[#2]

Departamento de Física. Universidad de Murcia.
E-30071 Murcia. Spain.

Abstract

We perform a non-perturbative chiral study of the masses of the lightest pseudoscalar mesons. In the calculation of the self-energies we employ the S-wave meson-meson amplitudes taken from Unitary Chiral Perturbation Theory (UCHPT) that include the lightest nonet of scalar resonances. Values for the bare masses of pions and kaons are obtained, as well as an estimate of the mass of the η_8. The former are found to dominate the physical pseudoscalar masses. We then match to the self-energies from Chiral Perturbation Theory (CHPT) to $\mathcal{O}(p^4)$, and a robust relation between several $\mathcal{O}(p^4)$ CHPT counterterms is obtained. We also resum higher orders from our calculated self-energies. By taking into account values determined from previous chiral phenomenological studies of $m_s/\hat{m}$ and $3L_7+L_8^r$, we determine a tighter region of favoured values for the $\mathcal{O}(p^4)$ CHPT counterterms $2L_6^r-L_4^r$ and $2L_8^r-L_5^r$. This determination perfectly overlaps with the recent determinations to $\mathcal{O}(p^6)$ in CHPT. We warn about a likely reduction in the value of $m_s/\hat{m}$ by higher loop diagrams and that this is not systematically accounted for by present lattice extrapolations. We also provide a favoured interval of values for $m_s/\hat{m}$ and $3L_7+L_8^r$.

[#1] email: oller@um.es
[#2] email: luisroca@um.es

1 Introduction

Chiral Perturbation Theory (CHPT) is the effective quantum field theory of strong interactions at low energies [1, 2, 3]. Three flavour CHPT, including strangeness, has already reached a very sophisticated stage with present calculations at the level of next-to-next-to-leading order (NNLO) or $\mathcal{O}(p^6)$ [4, 5, 6]. In ref.[7, 8] the masses and decay constants of the lightest octet of pseudoscalar mesons are worked out at to $\mathcal{O}(p^6)$. In this reference it is shown that the $\mathcal{O}(p^6)$ two loop contributions to the self-energies of the pseudoscalars are much larger than the full $\mathcal{O}(p^4)$. In addition, the $\mathcal{O}(p^6)$ tree level contributions to the kaon and eta masses, with the $\mathcal{O}(p^6)$ chiral counterterms estimated by resonance saturation, are much larger in modulus than the $\mathcal{O}(p^6)$ pure loop ones and with opposite sign. As stated in ref.[8] the $\mathcal{O}(p^6)$ counterterms "seem severely overestimated" due to the complicated nature of the scalar sector. Hence, this reference rises the interesting question of how one can improve the calculation of the contributions from the lightest scalar resonances. It is well known that the scalar sector is a source of large higher order corrections to the CHPT series. As a relevant example, let us quote the $I = 0$ $\pi\pi$ scattering length, a_0^0, which receives large higher order corrections (a 40% correction with respect to the lowest order value). This should be compared with the *non-resonant* $I = 2$ S-wave scattering length, a_0^2, which has negligible higher order corrections [9, 10, 11]. Even larger higher order chiral corrections due to the $I = 0$ S-wave final state interactions happen for the lowest order prediction of $\Gamma(\eta \to 3\pi)$, more than a factor of 2 [12, 13]. Another good example is the process $\gamma\gamma \to \pi^0\pi^0$ for which a two-loop CHPT calculation is needed [14, 15] to improve the comparison with dispersive theory calculations [16, 17, 18]. In connection with these enhancements one has the *generation* of the lightest scalar resonances σ, $f_0(980)$, $a_0(980)$ and κ [19, 20, 21, 22] because of the self-interactions among the pseudoscalars in S-wave.

The Feynman-Hellman theorem [23] relates $\partial M^2/\partial m_q$, where M is a hadronic mass and m_q the q quark mass, with the $\bar{q}q$ scalar form factor of this hadron at zero four-momentum transfer, the so called sigma-terms [24]. Of special relevance are those in connection with the lightest hadronic states, π, K, η for mesons and the nucleon for baryons. The large impact on the evaluation of the pion-nucleon sigma-term of the $I = J = 0$ $\pi\pi$ amplitude, due to the t-channel $\pi\pi$ exchange, is remarked in ref.[25]. On the other hand, it was stressed in refs.[26, 27, 28, 29] that the scalar form factor of the pion receives large unitarity corrections so that the one-loop CHPT approximation becomes inaccurate at a surprisingly low energy. Here, the so called infrared singularities are enhanced in comparison e.g. with the vector form factor [27, 20]. In ref.[29] the scalar $K\bar{K}$ form factors were first evaluated at the one loop level in CHPT and also employed in UCHPT. The corrections to these form factors because of the final state interactions of the $I = J = 0$ $\pi\pi$ and $K\bar{K}$ coupled channels were huge, see figs. 5 and 6 of ref.[29]. Since this happens to the scalar form factors one should expect a similar large impact of the $I = J = 0$ pseudoscalar-pseudoscalar amplitudes in evaluating the pseudoscalar masses, as both quantities are related by the Feynman-Hellman theorem. We offer here an estimation of such effects, that includes the exchanges of the lightest scalar resonances σ, κ, $f_0(980)$ and $a_0(980)$.

Recently, precise calculations of the pseudoscalar masses in lattice QCD with three dynamical fermions are available [30, 31, 32]. In these evaluations lattice results are taken down to the values of the lightest quark masses, m_u and m_d, and extrapolated to the continuum by employing perturbative SU(3) Staggered CHPT calculations [33, 34]. Given the large size of the pure loop contributions at $\mathcal{O}(p^6)$ estimated in ref.[8], and since they were neglected in refs.[31, 32], one should consider the possibility whether these large contributions are buried in the present values for quark masses and low energy parameters determined by this Collaboration.

The manuscript is organized as follows. Section 2 is dedicated to the development of the formalism for the calculation of the self-energies. In section 3 the results without matching with CHPT at $\mathcal{O}(p^4)$ are given, this is what we call the full dynamical self-energies. The $\mathcal{O}(p^4)$ CHPT self-energies are introduced and supplemented with higher order corrections from our formalism in section 4. We also derive in this section a robust relation between $L_{(4,6)} = 2L_6^r - L_4^r$ and $L_{(5,8)} = 2L_8^r - L_5^r$ and determine our interval of values for these counterterms. It turns out that this region remarkably overlaps with the values determined in refs.[35, 7] from $\mathcal{O}(p^6)$ fits to data. We discuss in section 5 about likely effects from higher loop diagrams and determine the values of $m_s/\hat{m}$, $L_{(7,8)} = 3L_7 + L_8^r$, and self-energies from our favoured region of low energy chiral counterterms. Some conclusions are collected in section 6.

2 Formalism

Our starting point is the S-wave meson-meson partial waves both for the resonant $I = 0$, 1 and 1/2, as well as for the much smaller and non-resonant ones, $I = 3/2$ and 2. For the former set we take the amplitudes of ref.[20]. The interaction kernel employed in this reference comprises the lowest order CHPT amplitudes together with the s-channel exchange of scalar resonances in a chiral symmetric invariant way from ref.[36]. These tree level resonances constitute an octet with mass around 1.4 GeV and a singlet around 1 GeV. On the other hand, the coupled channels are $\pi\pi$, $K\overline{K}$ and $\eta\eta$ for $I = 0$, $\pi\eta$ and $K\overline{K}$ for $I = 1$ and $K\pi$ and $K\eta$ for $I = 1/2$. In addition to the resonances explicitly included at tree level, related to the physical ones around 1.4 GeV like e.g. the $K_0^*(1410)$ or the $a_0(1450)$, the approach also generates dynamically the resonances σ or $f_0(600)$, κ, $a_0(980)$ and the main contribution to the $f_0(980)$. These resonances are generated even when no explicit resonances at tree level are included. The basic point in UCHPT is to resum the right hand or unitarity cut to all orders, the source of the large corrections produced by the S-wave meson-meson interactions, and perform a chiral expansion of the rest, the so called interaction kernel [37, 38, 20]. For the non-resonant isospins 3/2 and 2, not given in ref.[20], the kernels correspond to the $\mathcal{O}(p^2)$ CHPT amplitudes. In fig.1 we show the reproduction of scattering data that is achieved by our S-wave amplitudes.

We only consider the S-waves since the lightest pseudoscalar self-energies are expected to be dominated by low energy physics where the P-waves are kinematically suppressed by small factors of three-momentum squared. This is true even in the calculations of loops since, after proper renormalization, the typical momentum in virtual processes will be bounded and of the same order as the on-shell values. Indeed, by a comparison of the order of magnitude of our results with those obtained by regularizing the loops with a three-momentum cut-off, the latter must be around $0.3 - 0.4$ GeV. At such energies only S-waves matters in very good approximation, which is also clear experimentally. Another signal of the suppression of P-wave dynamics in the self-energies is the fact that it only starts to contribute at the two chiral loop level. In addition, we recall the discussion in section 1 concerning the large corrections to the chiral series typically induced by the resonant S-wave channels and the large $\mathcal{O}(p^6)$ counterterms calculated from resonance exchanges in ref.[8].

There is recently both experimental and theoretical overwhelming evidence of the existence of the $I = 0$ σ [39, 19, 20, 40, 41, 42] and $I = 1/2$ κ [39, 20, 40, 21, 42, 43] resonances. One also has the $I = 0$ resonance $f_0(980)$ and the $I = 1$ $a_0(980)$. These resonances have been considered quite often in the literature to form the lightest nonet of scalar resonances [44, 20, 40, 45], though there is not still consensus on this issue. Since these resonances are the lightest scalar ones it is an interesting question to calculate their contributions to the pseudoscalar masses. In connection with this, we plot in fig.2 those contributions to the pseudoscalar self-energies that follow from the exchange of scalar resonances R at the level of one loop with dressed propagators.[#3]

[#3] There is a similar contribution to that of fig.2b with the resonance leg coupling directly to the vacuum without the tadpole in the upper extreme for the preexisting octet of scalar resonances at 1.4 GeV. These contributions were included e.g. in ref.[21, 46] and their contributions to the chiral series for evaluating self-energies are negligible as they only contribute

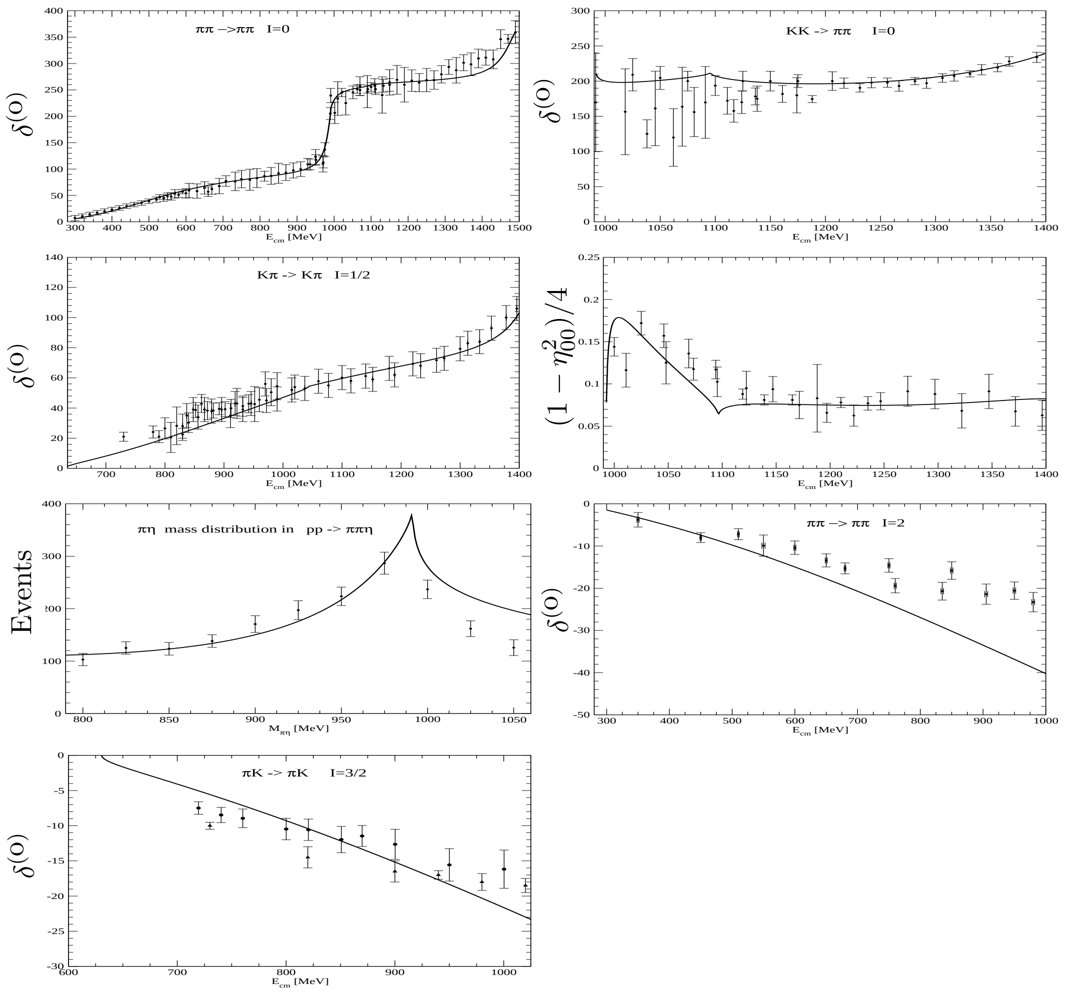

Figure 1: Different phase-shifts, inelasticities and mass distributions obtained with the unitarized amplitudes. The experimental data are from refs. [47, 48, 49, 50, 51, 52, 53, 54, 55, 56, 57, 58, 59]

Within UCHPT [20] the resonances $f_0(980)$, $a_0(980)$, σ, κ and an octet around 1.4 GeV appear as poles of the corresponding S-wave amplitudes once the right hand cut is resummed according to fig.3a. In this way fig.2a is included in the evaluation of fig.3b and, analogously, fig.2b is a contribution in fig.4b. As remarked above, the lightest scalar resonances are generated through the self-interactions of the pseudoscalars [19, 20], with the kernel given by Chiral Symmetry [1, 2, 3]. These scalar resonances in figs.2 better correspond to two pseudoscalars strongly correlated by the strong self-interactions. Hence, in order to avoid double-counting one cannot talk independently of the contributions of the unitarity loops and the light scalar resonances. Both must be calculated at once. This is why a scheme like that in figs.3 and 4 is the appropriate one. For the resonances higher in mass, namely, the octet around 1.4 GeV, the situation is quite different as they are preexisting resonances that are dressed by the interaction with the pseudoscalars. In this way, tree level exchanges and pseudoscalar loops can be differentiated in a perturbative way of thinking.

For the calculation of fig.3b we proceed by analogy with fig.2a. Note that in ref.[60] it was shown

---

to $2L_8^r - L_5^r$ and $2L_6^r - L_4^r$, modulo small higher order contributions, with a vanishing result.

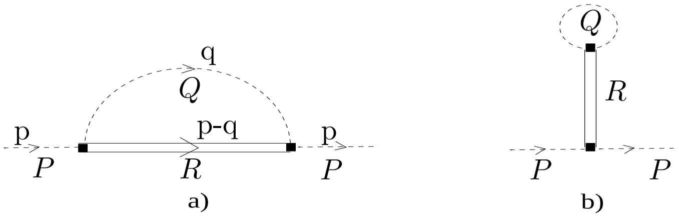

Figure 2: Fig.2a represents the $s-$channel exchange of scalar resonances R in terms of the intermediate Q and initial P pseudoscalars. A sum over all possible intermediate Q and R should be understood. The fig.2b corresponds to the crossed exchange of the $I = 0$ scalar resonances R.

that the pion and $K\pi$ scalar form factors are dominated by the Laurent poles of the σ and κ resonances, respectively, for energies below the next resonance. In the case of the $I = 0$ and $1/2$ S-waves it was similarly shown that they are given by the previous poles plus a background, which mainly consists of just a constant which would give rise to a term analogous to fig.2b or 4b. It follows then that fig.2a is a close analogy to fig.3b. After performing the integration over the null component of q in the loop, see fig.2a, one has two type of cuts. The first corresponds to having the pseudoscalar Q on-shell, while for the second the state on-shell is $\overline{R}$, running with opposite sense to that of R. The former involves the $P\overline{Q}$ scalar interaction mediated by the scalar resonance R. This is the contribution we are seeking. The latter corresponds to the $P\overline{R}$ pseudoscalar interaction mediated by the pseudoscalar Q which is wildly off-shell and suppressed because the resonance energy is $-E_R$.

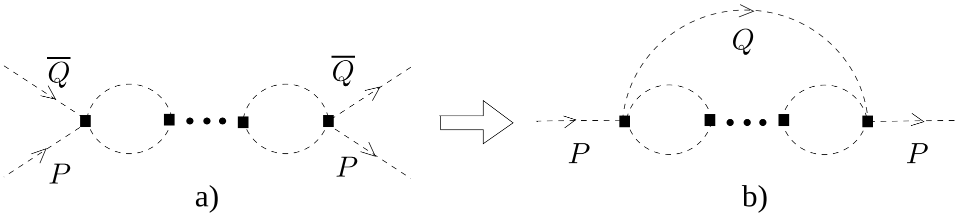

Figure 3: Fig.3a represents the S-wave amplitude $P\overline{Q} \to P\overline{Q}$ and fig.3b is the diagram for the calculation of the self-energy of the pseudoscalar P due to the intermediate pseudoscalar Q.

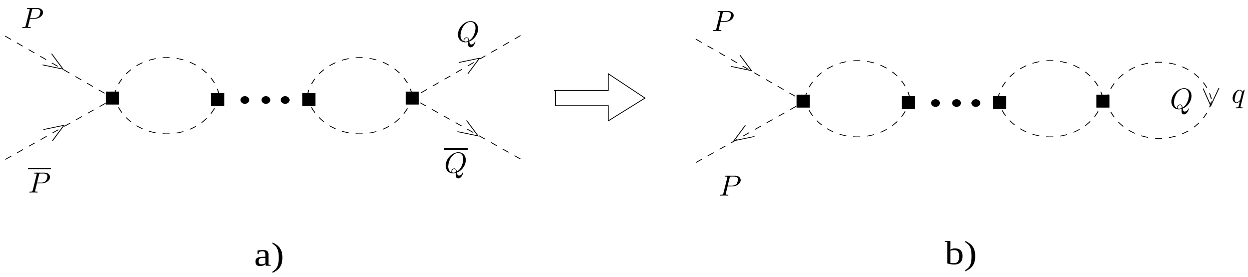

Figure 4: Tadpole diagram for the self-energy of the pseudoscalar P.

We then isolate from figs.2a and 3b the following scalar contribution to the self-energies of the pseudoscalars,

$$\Sigma_P^U = -\sum_Q \int \frac{d^3k}{(2\pi)^3 2E_Q(\mathbf{k})} T_{P\overline{Q}\to P\overline{Q}}(s_1) \ . \tag{2.1}$$

with $Q = \{\pi^+, \pi^-, \pi^0, K^+, K^-, K^0, \overline{K}^0, \eta\}$ and $s_1 = (M_P - E_Q(\mathbf{k}))^2 - \mathbf{k}^2$ for $p = (M_P, \vec{0})$. The previous equation is invariant under Lorentz transformation as must be the case for a self-energy because a meson-meson scattering amplitude is a Lorentz scalar. The sum in eq.(2.1) is over all the species of pseudoscalars because all of them give rise to different $P\overline{Q}_i \to P\overline{Q}_i$ amplitudes.

As stated above, one also has the corresponding diagrams figs.2b and 4b. Notice that in fig.3 we were driven to consider the amplitudes $P\overline{Q}_i \to P\overline{Q}_i$, but one has to take into account the $t-$crossed process $P\overline{P} \to Q_i\overline{Q_i}$ as well. We can evaluate the diagram in fig.4b by performing the contour integration for q^0. Here one only has the singularity due to the Q pseudoscalar and,

$$\Sigma_P^{tad} = -\sum_{Q=\pi^0,\pi^+,K^+,K^0,\eta} \lambda_Q \int \frac{d^3k}{(2\pi)^3 2E_Q(\mathbf{k})} T_{P\overline{P}\to Q\overline{Q}}(0) \ . \tag{2.2}$$

In Σ_P^{tad} one sums only over particles (without including the sum over antiparticles) since in the final state both particles and antiparticles happen and otherwise one is double-counting. Finally, $\lambda_Q = 1$ for π^+, K^+ and K^0 and $\lambda_Q = 1/2$ for π^0 and η, because they are their own antiparticles. These warnings also happen in the standard calculations of tadpoles with the use of Feynman rules because of the same reasons. The self-energy of the pseudoscalar P is then given by the sum,

$$\Sigma_P = \Sigma_P^U + \Sigma_P^{tad} \ , \tag{2.3}$$

In terms of the amplitudes for the different channels we have for the π, K and η self-energies,

$$\begin{aligned}
\Sigma_\pi &= -\int \frac{d^3k}{(2\pi)^3 2E_Q(\mathbf{k})} \Big[\frac{10}{3} T^{I=2}_{\pi\pi\to\pi\pi}(s) + \frac{2}{3} T^{I=0}_{\pi\pi\to\pi\pi}(s) + \frac{8}{3} T^{I=3/2}_{\pi\bar{K}\to\pi\bar{K}}(s) + \frac{4}{3} T^{I=1/2}_{\pi\bar{K}\to\pi\bar{K}}(s) + T^{I=1}_{\pi\eta\to\pi\eta}(s) \\
&+ T^{I=0}_{\pi\pi\to\pi\pi}(0) + \frac{2}{\sqrt{3}} T^{I=0}_{\pi\pi\to K\bar{K}}(0) - \frac{1}{\sqrt{3}} T^{I=0}_{\pi\pi\to\eta\eta}(0) \Big] \\
\Sigma_K &= -\int \frac{d^3k}{(2\pi)^3 2E_Q(\mathbf{k})} \Big[2T^{I=3/2}_{\pi K\to\pi K}(s) + T^{I=1/2}_{\pi K\to\pi K}(s) + \frac{3}{2} T^{I=1}_{K\bar{K}\to K\bar{K}}(s) + \frac{1}{2} T^{I=0}_{K\bar{K}\to K\bar{K}}(s) \\
&+ \frac{3}{2} T^{I=1}_{KK\to KK}(s) + \frac{1}{2} T^{I=0}_{KK\to KK}(s) + T^{I=1/2}_{K\eta\to K\eta}(s) \\
&+ \frac{\sqrt{3}}{2} T^{I=0}_{K\bar{K}\to\pi\pi}(0) + T^{I=0}_{K\bar{K}\to K\bar{K}}(0) - \frac{1}{2} T^{I=0}_{K\bar{K}\to\eta\eta}(0) \Big] \\
\Sigma_\eta &= -\int \frac{d^3k}{(2\pi)^3 2E_Q(\mathbf{k})} \Big[3T^{I=1}_{\pi\eta\to\pi\eta}(s) + 4T^{I=1/2}_{\eta K\to\eta K}(s) + 2T^{I=0}_{\eta\eta\to\eta\eta}(s) \\
&- \sqrt{3} T^{I=0}_{\eta\eta\to\pi\pi}(0) - 2T^{I=0}_{\eta\eta\to K\bar{K}}(0) + T^{I=0}_{\eta\eta\to\eta\eta}(0) \Big]
\end{aligned} \tag{2.4}$$

Notice that we are employing just the S-wave contribution to the full strong amplitude T_{ij}, and this is why we have kept only the s-Mandelstam variable in the argument of $T_{ij}(s_1)$, dropping the t dependence in eq.(2.4). This is what automatically occurs when considering the intermediate scalar resonances in figs.2a, b. The Clebsch-Gordan coefficients in front of the S-wave amplitudes in the previous equations are obtained from a standard isospin analysis. As an example, for the π^+ self-energy one has the S-wave amplitudes,

$$
\begin{aligned}
T_{\pi^+\pi^-\to\pi^+\pi^-}+T_{\pi^+\pi^+\to\pi^+\pi^+}+T_{\pi^+\pi^0\to\pi^+\pi^0} &= \left(\frac{1}{6}T^{I=2}_{\pi\pi\to\pi\pi}+\frac{1}{3}T^{I=0}_{\pi\pi\to\pi\pi}\right)+T^{I=2}_{\pi\pi\to\pi\pi}+\frac{1}{2}T^{I=2}_{\pi\pi\to\pi\pi} \\
&= \frac{5}{3}T^{I=2}_{\pi\pi\to\pi\pi}+\frac{1}{3}T^{I=0}_{\pi\pi\to\pi\pi}\ . \qquad (2.5)
\end{aligned}
$$

To finally obtain the coefficients in Σ_π one has to multiply by 2 the $T^I_{\pi\pi\to\pi\pi}$ S-waves in the last expression because in refs.[19, 20] one uses the $I=0,\,2$, $\pi\pi$ states (and also the $I=0$ $\eta\eta$ one) normalized to 1/2. In this way, these symmetric states under the exchange of the two pions can be treated as if the latter were distinguishable. For more details see refs.[19, 20].

The integral in eq.(2.1) for Σ_P^U is ultraviolet divergent since for large three-momentum the measure grows as $\mathbf{k}^2$ and $T_{P\overline{Q}\to P\overline{Q}}(s_1)$ tends to $1/\log s_1$ or constant for $|s_1|\to\infty$. This, together with the factor $E_Q(\mathbf{k})$ in the denominator, gives rise to a quadratic divergence. For Σ_P^{tad}, eq.(2.2), one has the same type of divergence as $T_{P\overline{P}\to Q\overline{Q}}$ is evaluated at $s_1=0$ and it is a constant.

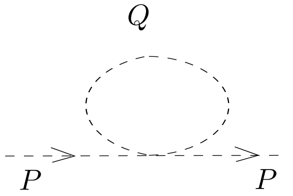

Figure 5: The one loop contribution of figs.3b and 4b at $\mathcal{O}(p^4)$. This is the only loop appearing at $\mathcal{O}(p^4)$ CHPT.

A general coupled channel S-wave T-matrix has the structure [20],

$$T=[I+\mathcal{K}\cdot G]^{-1}\cdot\mathcal{K}\ , \qquad (2.6)$$

with $\mathcal{K}$ the interaction kernel and G corresponds to the unitarity bubbles shown in fig.3. For more details see ref.[20]. The previous equation has the expansion,

$$T=[I-\mathcal{K}\cdot G+\mathcal{K}\cdot G\cdot\mathcal{K}+\ldots]\cdot\mathcal{K}\ . \qquad (2.7)$$

We notice that when $T=\mathcal{K}_2$ (the lowest order CHPT amplitudes), one has no unitarity bubbles in fig.3b and fig.4b, and then both figures give the same diagram. This only happens for $\mathcal{K}_2$ at lowest order in CHPT. The local term $\mathcal{K}_2$ gives rise to the one loop diagram shown in fig.5, the only one that appears at next-to-leading order (NLO) in CHPT (at this order the rest of contributions come from local counterterms [2, 3]). In order to avoid this double-counting we then subtract the contribution in fig.5 to the integral in eq.(2.1), fig.3b. This is done explicitly below in eq.(2.27).

2.1 Regularization and renormalization

We now proceed with the evaluation of the integral in eq.(2.1) for Σ_P^U. The integral in eq.(2.2) for Σ_P^{tad} is a particular case of the previous one. Firstly, we perform the angular integration and change to the energy as the integration variable.

$$\int\frac{d^3k}{(2\pi)^3 2E_Q(\mathbf{k})}T_{P\overline{Q}\to P\overline{Q}}(s_1)=\int_{M_Q}^{\infty}\frac{|\mathbf{k}|dE_Q}{4\pi^2}T_{P\overline{Q}\to P\overline{Q}}(s_1)\ . \qquad (2.8)$$

We now introduce the new variable

$$t = M_Q/E_Q \ . \tag{2.9}$$

As the resulting integral diverges quadratically for $t \to 0$, we change the lower limit to ε, positive and small, taking at the end the limit $\varepsilon \to 0^+$.

$$\frac{M_Q^2}{(2\pi)^2} \int_\varepsilon^1 dt \frac{\sqrt{1-t^2}}{t^3} T_{P\overline{Q}\to P\overline{Q}}(s_1) \ , \tag{2.10}$$

with $s_1 = M_P^2 + M_Q^2 - 2M_P M_Q/t$. Notice that since $\varepsilon = M_Q/\Lambda$, with $\Lambda \gg M_Q$ being the upper limit in the three-momentum of eq.(2.8), the previous limit is equivalent to $\Lambda \to +\infty$. In performing this limit we must identify those terms that scales as $1/\varepsilon^2$, $1/\varepsilon$ (equivalently as Λ^2, Λ) and remove them from the result. In order to remove infinities one must work out algebraic expressions for the previous integral that explicitly show these diverging powers of ε. The problem of accomplishing this aim is the complicated matrix expression for the strong amplitude that prevents us from giving a close expression for the integral in eq.(2.10). However, we are interested in isolating algebraically the dependence in ε, and this can be done by performing a dispersion relation representation for $T_{P\overline{Q}\to P\overline{Q}}(s_1)$ in the physical Riemann sheet.

The $T_{P\overline{Q}\to P\overline{Q}}(s_1)$ amplitude from ref.[20] has only one cut, the right or unitarity one, and tends to $1/\log s_1$ or constant when $s_1 \to \infty$. In order to perform the dispersion relation we take as integration contour a circle in the infinity deformed to engulf the real axis along the right hand cut, $s_{th} < s_1 < \infty$, with s_{th} the lightest meson-meson threshold with the $P\overline{Q}$ S-wave quantum numbers. We take one subtraction because of the aforementioned behaviour of $T_{ij}(s_1)$ at infinity. We then have:

$$T_{ij}(s_1) = T_{ij}(s_2) + \frac{s_1 - s_2}{\pi} \int_{s_{th}}^\infty ds' \frac{\text{Im}T_{ij}(s')}{(s'-s_1)(s'-s_2)} + \sum_{\ell=1}^N \frac{(s_2 - s_1)R_{ij}^{(\ell)}}{(s_\ell^R - s_1)(s_\ell^R - s_2)} \ , \tag{2.11}$$

with s_2 the point where the subtraction has been performed. In addition, N is the number of poles of $T_{ij}(s)$ in the physical Riemann sheet and $R_{ij}^{(\ell)}$ is the residue of the ℓ_{th} pole at the position s_ℓ^R. Because of the Schwartz reflection principle any partial wave satisfies that $T_{ij}(s^*) = T_{ij}(s)^*$, so that poles always appear as pairs in relative complex conjugate positions with complex conjugate residua. Taking then s_2 real in eq.(2.11) the contribution from the sum of poles is real for s_1 along the real s-axis.

A physical partial wave should not have any pole on the physical sheet with non-vanishing imaginary part. But notice that the lowest order CHPT S-wave amplitudes in $I = 1/2$ ($K\pi \to K\pi$, $K\pi \to K\eta$ and $K\eta \to K\eta$) have each of them one pole at $s = 0$ due to the kinematical reason of having different masses, see ref.[20] for explicit expressions of those amplitudes. This pole at $s = 0$ for the interaction kernel drives the appearance of a pole in the final $K\pi \to K\pi$ S-wave for a real s value, typically at around $s = -0.25$ GeV^2, not far away from its lowest order value. This poles gives rise to a non-negligible effect in the calculation of the π self-energy. There are also other poles with non-zero imaginary part. Reassuringly, these poles are always far away of the physical axis and their contributions to the pseudoscalar self-energies are negligible, as we have numerically checked.

Let us proceed with the evaluation of the renormalized value of the divergent integral eq.(2.10) making use of the representation given in eq.(2.11) for the S-wave T-matrix elements. Both the contributions from the unitarity cut and poles involve the same sort of integral,

$$J(s', s_2) = \int_\varepsilon^1 dt \frac{\sqrt{1-t^2}}{t^3} \frac{s_1(t) - s_2}{s' - s_1(t)} \ . \tag{2.12}$$

For the sum over the poles in eq.(2.11) the variable s' must be replaced by s_ℓ^R. For convenience, new variables a and b are introduced,

$$a = \nu - \frac{s_2}{2M_P M_Q} \ , \ b = \nu - \frac{s'}{2M_P M_Q} \ , \tag{2.13}$$

with $\nu = (M_P^2 + M_Q^2)/(2M_P M_Q)$. Notice that one can also write $1/t = \nu - s_1/2M_P M_Q$. Then,

$$\begin{aligned} J(s', s_2) &= -\int_\varepsilon^1 dt \frac{\sqrt{1-t^2}}{t^3} \frac{1-at}{1-bt} = -\int_\varepsilon^1 \frac{\sqrt{1-t^2}}{t^3} + (a-b)\int_\varepsilon^1 dt \frac{\sqrt{1-t^2}}{t^2} \\ &+ (a-b)b \int_\varepsilon^1 dt \frac{\sqrt{1-t^2}}{t} - (a-b)b \int_\varepsilon^1 dt \frac{\sqrt{1-t^2}}{t-1/b} \ . \end{aligned} \tag{2.14}$$

The first integral is elementary, although its renormalized value requires some comments.

$$-\int_\varepsilon^1 dt \frac{\sqrt{1-t^2}}{t^3} = -\frac{1}{2}\frac{\sqrt{1-\varepsilon^2}}{\varepsilon^2} + \frac{1}{2}\log \frac{1+\sqrt{1-\varepsilon^2}}{\varepsilon} \ . \tag{2.15}$$

Now, when sending $\varepsilon \to 0^+$ both terms on the r.h.s. diverge. Performing a power series around $\varepsilon = 0$ one has $-1/2\varepsilon^2 + (1 - 2\log\varepsilon/2)/4 + \mathcal{O}(\varepsilon^2)$. The first term in this sum diverges like ε^{-2} and should be reabsorbed by appropriate chiral counterterms. The terms with positive powers of ε, not explicitly shown, vanish for $\varepsilon \to 0$. Then, the remaining contribution is,

$$\frac{1}{4}\left(1 - 2\log\frac{M_Q}{2\Lambda}\right) = \frac{1}{4}\left(1 - 2\log\frac{M_Q}{2\mu}\right) - \frac{1}{2}\log\frac{\mu}{\Lambda} \ , \tag{2.16}$$

where the renormalization scale μ is introduced. In sending $\Lambda \to +\infty$ ($\varepsilon \to 0^+$), again the term $\log\mu/\Lambda$ diverges and should be reabsorbed by the appropriate counterterms. Then one has:

$$-\int_0^1 dt \frac{\sqrt{1-t^2}}{t^3} \doteq \frac{1}{4}\left(1 - 2\log\frac{M_Q}{2\mu}\right) \ , \tag{2.17}$$

where the symbol $\doteq$, used for expressing our renormalized integrals, means equal up to terms divergent as ε^{-2}, ε^{-1} or $\log\varepsilon$, when $\varepsilon \to 0^+$. When giving our results we shall vary μ between 0.5 and 1.2 GeV, providing in this way an estimate of possible constants of order one that may change depending on the renormalization scheme chosen. E.g. the difference between our procedure and the results in the modified $\overline{MS}$ scheme in dimensional regularization used in CHPT [2, 3]. This variation in μ will be a source of uncertainty in our results and it will be consider in the error analyses. In ref.[39] the unitarity bubble G in eq.(2.6) was also calculated within a cut-off scheme. If one sends this cut-off to infinity only a logarithmic divergence remains, as we have here. By varying μ within the range mentioned above, one is accounting for finite constant terms, like the subtraction constant used in G.

The second and third integrals on the right hand side of eq.(2.14) can be treated similarly. For the last one,

$$\int dt \frac{\sqrt{1-t^2}}{t-c} = \sqrt{1-t^2} - c \arcsin t + (1-c^2)\int \frac{dt}{(t-c)\sqrt{1-t^2}} \ , \tag{2.18}$$

with $c = 1/b$ and

$$\widetilde{I}(b) = \int_\varepsilon^1 \frac{dt}{(t-1/b)\sqrt{1-t^2}} \quad = \quad i) \ \frac{1}{\sqrt{1-1/b^2}} \log\frac{1+\sqrt{1-1/b^2}}{\varepsilon + 1/b} \ , \ b > 1 \ ,$$

$$
\begin{aligned}
&ii)\ \frac{1}{\sqrt{1-1/b^2}}\log\frac{1+\sqrt{1-1/b^2}}{\varepsilon-1/b}\ ,\ b<-1\ ,\\
&iii)\ \frac{-1}{\sqrt{1/b^2-1}}\left(\frac{\pi}{2}+\arcsin b\right)\ ,\ 0<b<1\ ,\\
&iv)\ \frac{1}{\sqrt{1/b^2-1}}\left(\frac{\pi}{2}+\arcsin b\right)\ ,\ -1<b<0\ ,
\end{aligned}
\tag{2.19}
$$

Adding all the integrals that contribute in eq.(2.14),

$$
J(s',s_2)=\frac{1}{4}+\frac{1}{2}\log\frac{2}{\varepsilon}+(a-b)b\log\frac{2}{\varepsilon}-(a-b)b(1-1/b^2)\,\widetilde{I}(b)\ . \tag{2.20}
$$

Now, in the expressions given for $\widetilde{I}$ with $|b|>1$ in eq.(2.19), the first two lines, one has $\log(\varepsilon+1/|b|)=\log\varepsilon+\log(1+1/\varepsilon|b|)$. This last term gives rise to an infinite series of divergent terms in powers of $1/(|b|\,\varepsilon)^n$ for $|b|>1$, equivalently in powers of $(\Lambda/b)^n$, which are removed in the regularization process. Substituting also $\log\varepsilon$ by $\log M_Q/\mu$, introducing the renormalization scale μ, as explained before, then

$$
\begin{aligned}
&J(s',s_2)\doteq\\
i)\quad &J_+(a,b)=\frac{1}{4}+\frac{1}{2}\log\frac{2\mu}{M_Q}+(a-b)b\log 2-(a-b)b(1-\sqrt{1-1/b^2})\log\frac{M_Q}{\mu}\\
&-(a-b)b\sqrt{1-1/b^2}\log(1+\sqrt{1-1/b^2})\ ,\ |b|>1\ ,\\
ii)\quad &J_-(a,b)=\frac{1}{4}+\frac{1}{2}\log\frac{2\mu}{M_Q}+(a-b)b\log\frac{2\mu}{M_Q}-(a-b)\sqrt{1-b^2}\left(\frac{\pi}{2}+\arcsin b\right)\ ,\ |b|<1\ .
\end{aligned}
\tag{2.21}
$$

The dispersive integral contribution to the self-energy of the pseudoscalar P by the intermediate Q is:

$$
\begin{aligned}
&I^{PQ}_{disp}=\int_\varepsilon^1 dt\frac{\sqrt{1-t^3}}{t^3}\frac{s_1-s_2}{\pi}\int_{s_{th}}^\infty ds'\frac{\mathrm{Im}T_{ij}(s')}{(s'-s(t))(s'-s_2)}\doteq\\
&i)\ \text{If }(M_P-M_Q)^2>s_{th}\\
&\frac{1}{\pi}\int_{s_{th}}^{(M_P-M_Q)^2}ds'\frac{\mathrm{Im}T_{ij}(s')}{(s'-s_2)}J_+(s',s_2)+\frac{1}{\pi}\int_{(M_P-M_Q)^2}^{(M_P+M_Q)^2}ds'\frac{\mathrm{Im}T_{ij}(s')}{(s'-s_2)}J_-(s',s_2)\\
&+\frac{1}{\pi}\int_{(M_P+M_Q)^2}^{+\infty}ds'\frac{\mathrm{Im}T_{ij}(s')}{(s'-s_2)}J_+(s',s_2)\\
&ii)\ \text{If }(M_P-M_Q)^2<s_{th}\\
&\frac{1}{\pi}\int_{s_{th}}^{(M_P+M_Q)^2}ds'\frac{\mathrm{Im}T_{ij}(s')}{(s'-s_2)}J_-(s',s_2)+\frac{1}{\pi}\int_{(M_P+M_Q)^2}^{+\infty}ds'\frac{\mathrm{Im}T_{ij}(s')}{(s'-s_2)}J_+(s',s_2)
\end{aligned}
\tag{2.22}
$$

Notice that $(M_P+M_Q)^2\geq s_{th}$. Let us remark that $J_+(s',s_2)$ vanishes like $-1/s'$ for $s'\to\infty$, as it is clear from eq.(2.21). This is why all the last integrals in the previous equations converge for $s'\to+\infty$.

The subtraction constant in eq.(2.11), $T_{ij}(s_2)$, contributes as,

$$
I^{PQ}_{subs}=T_{ij}(s_2)\int_\varepsilon^1 dt\frac{\sqrt{1-t^2}}{t^3}\doteq -T_{ij}(s_2)\frac{1}{4}\left(1-2\log\frac{M_Q}{2\mu}\right)\ , \tag{2.23}
$$

from eq.(2.17). The contribution of the sum of poles in eq.(2.11) is:

$$
I^{PQ}_{pole}=-\sum_{\ell=1}^{N}\frac{R^{(\ell)}_{ij}}{(s^R_\ell-s_2)}J_+(a,b(s^R_\ell))\ . \tag{2.24}
$$

We have only $J_+(a,b)$ since for this case always $|b|>1$ as the poles happen far away in the complex plane or on the negative s-axis. If s_2 is taken such that $a=0$ then $J(a,b)$ will vanish like $\mathcal{O}(b^{-2})$ for $|b|\to\infty$, as follows from eq.(2.21). One can take advantage of this fact since the pole contributions will tend to vanish because s_ℓ^R and the resulting $|b|$ are large. Thus, we fix $s_2=s_A=M_P^2+M_Q^2$ in the following so that $a=0$, eq.(2.13). This choice also makes that all the contributions in our final equation for the self-energies, eq.(2.29) below, have natural size.

One still has to remove the $\mathcal{O}(p^4)$ contribution to I_{disp}^{PQ} in order to avoid double-counting with the tadpole contribution, as explained above after eq.(2.7). We then evaluate eq.(2.1) with $T_{P\overline{Q}\to P\overline{Q}}$ given by its $\mathcal{O}(p^2)$ expression. A general CHPT S-wave amplitude at $\mathcal{O}(p^2)$ has the form,

$$T_{ij}^{(2)}(s)=A+Bs+\frac{C}{s}\ . \tag{2.25}$$

The last term in the sum only appears for the $I=1/2$ $K\pi$ and $K\eta$ coupled channel amplitudes involving two particles with different masses. Then,

$$\begin{aligned}&\int_0^1 dt\frac{\sqrt{1-t^2}}{t^3}\left(A+Bs_1(t)+\frac{C}{s_1(t)}\right)\\&=\int_0^1\frac{\sqrt{1-t^2}}{t^3}\left(A+s_AB\right)-2M_PM_QB\int_0^1 dt\frac{\sqrt{1-t^2}}{t^4}+\frac{C}{s_A}\int_0^1 dt\frac{\sqrt{1-t^2}}{t^2}\frac{1}{t-f}\ ,\end{aligned} \tag{2.26}$$

with $f=1/\nu$ ($f<1$ when $C\neq 0$) and $s_A=M_P^2+M_Q^2$. The renormalized second integral in this equation vanishes as can easily worked out. We then have,

$$\begin{aligned}I_{rem}^{PQ}&=T_{ij}^{(2)}(s_A)\int_0^1 dt\frac{\sqrt{1-t^2}}{t^3}+\frac{C}{s_A}\int_0^1 dt\frac{\sqrt{1-t^2}}{t^3}\frac{f}{t-f}\\&=-T_{ij}^{(2)}(s_A)\frac{1}{4}(1-2\log\frac{M_Q}{2\mu})+\frac{C}{s_A}J_+(0,1/f)\ .\end{aligned} \tag{2.27}$$

The other contribution to Σ_P is Σ_P^{tad}, eq.(2.3). Its calculation, eq.(2.15), is straightforward and gives,

$$I_{tad}^{PQ}=\lambda_Q T_{ij}(0)\int_\varepsilon^1 dt\frac{\sqrt{1-t^2}}{t^3}\doteq-\lambda_Q\frac{T_{ij}(0)}{4}\left(1-2\log\frac{M_Q}{2\mu}\right)\ . \tag{2.28}$$

Hence, for eq.(2.3) one has:

$$\Sigma_P=-\sum_Q\frac{M_Q^2}{(2\pi)^2}\left(I_{subs}^{PQ}+I_{disp}^{PQ}+I_{pole}^{PQ}-I_{rem}^{PQ}\right)-\sum_{Q'}\frac{M_{Q'}^2}{(2\pi)^2}I_{tad}^{PQ'} \tag{2.29}$$

with $Q=\{\pi^0,\pi^+,\pi^-,K^0,\overline{K}^0,K^+,K^-,\eta\}$ and $Q'=\{\pi^0,\pi^+,K^+,K^0,\eta\}$. Notice that after the subtraction of $\sum_Q I_{rem}^{PQ}M_Q^2/(2\pi)^2$ to the previous equation, the only contribution at $\mathcal{O}(p^4)$ of our result comes from $I_{tad}^{PQ}M_Q^2/(2\pi)^2$ when $T_{ij}(0)$ in eq.(2.28) is substituted by $T_{ij}^{(2)}(0)$, the corresponding lowest order CHPT amplitude. It is important to remark that for this $\mathcal{O}(p^4)$ case we have checked that $\sum_{Q'}I_{tad}^{PQ'}M_{Q'}^2/(2\pi)^2$ reproduces the CHPT infrared logarithms on the quark masses in CHPT at $\mathcal{O}(p^4)$ [3]. This is one among the many explicit calculations in the literature showing that by sending $\Lambda\to+\infty$ and removing the power divergences (which necessarily disappears in dimensional regularization) one recovers the dimensional regularization results with the differences reabsorbed in the chiral counterterms from the tree level contributions [61, 62, 63].

2.2 Mass equations

We often remove the $\mathcal{O}(p^4)$ contribution to Σ_P and denote by Σ_P^H the $\mathcal{O}(p^6)$ and higher order contributions. The latter is obtained with the replacement of $T_{ij}(0)$ by $T_{ij}(0) - T_{ij}^{(2)}(0)$ in eq.(2.28) for the tadpole contribution. The $\mathcal{O}(p^4)$ CHPT expressions for the pseudoscalar masses are, ref.[3]:

$$\begin{aligned}
M_\pi^2 &= \overset{\circ}{M}{}_\pi^2 \left\{1 + \mu_\pi - \frac{1}{3}\mu_\eta + 2\hat{m}K_3 + K_4\right\} ,\\
M_K^2 &= \overset{\circ}{M}{}_K^2 \left\{1 + \frac{2}{3}\mu_\eta + (\hat{m} + m_s)K_3 + K_4\right\} ,\\
M_\eta^2 &= \overset{\circ}{M}{}_\eta^2 \left\{1 + 2\mu_K - \frac{4}{3}\mu_\eta + \frac{2}{3}(\hat{m} + m_s)K_3 + K_4\right\} + \overset{\circ}{M}{}_\pi^2 \left\{-\mu_\pi + \frac{2}{3}\mu_K + \frac{1}{3}\mu_\eta\right\} + K_5 ,
\end{aligned} \tag{2.30}$$

where,

$$\begin{aligned}
K_3 &= \frac{8B_0}{F_0^2}(2L_8^r - L_5^r) \ , \ K_4 = (2\hat{m} + m_s)\frac{16B_0}{F_0^2}(2L_6^r - L_4^r) \ ,\\
K_5 &= (m_s - \hat{m})^2 \frac{128}{9}\frac{B_0^2}{F_0^2}(3L_7 + L_8^r) \ , \ \mu_Q = \frac{1}{32\pi^2}\frac{\overset{\circ}{M}{}_P^2}{F_0^2}\log\frac{\overset{\circ}{M}{}_P^2}{\mu^2} \ .
\end{aligned} \tag{2.31}$$

The symbol $\overset{\circ}{M}_P$ denotes the bare mass of the pseudoscalar P corresponding to the lowest order CHPT result,

$$\overset{\circ}{M}{}_\pi^2 = 2B_0\hat{m} \ , \quad \overset{\circ}{M}{}_K^2 = B_0(\hat{m} + m_s) \ , \quad \overset{\circ}{M}{}_\eta^2 = \frac{2}{3}B_0(\hat{m} + 2m_s) \ , \tag{2.32}$$

and B_0 measures the strength of the quark condensate $\langle 0|\bar{q}q|0\rangle = -F_0^2 B_0 + \mathcal{O}(m_q^2)$ in the SU(3) chiral limit. We will denote the $\mathcal{O}(p^4)$ CHPT self-energies by $\Sigma_P^{4\chi} = M_P^2 - \overset{\circ}{M}{}_P^2$, eq.(2.30). Notice that from eq.(2.32) $\overset{\circ}{M}{}_\eta^2$ always satisfies the Gell-Mann-Okubo mass relation,

$$\overset{\circ}{M}{}_\eta^2 = \frac{1}{3}(4\,\overset{\circ}{M}{}_K^2 - \overset{\circ}{M}{}_\pi^2) \ . \tag{2.33}$$

On the other hand, the L_i^r coefficients are the renormalized values of the low energy CHPT counterterms at $\mathcal{O}(p^4)$ from ref.[3] within the $\overline{MS} - 1$ scheme.

The mass equation one has to solve is,

$$M_P^2 = \overset{\circ}{M}{}_P^2 + \Sigma_P(\overset{\circ}{M}{}_Q^2; M_Q^2) \ , \tag{2.34}$$

with Σ_P given in eq.(2.29). The dependence on the bare masses $\overset{\circ}{M}{}_Q^2$ originates from the one of the interaction kernel $\mathcal{K}$ [20].

If we impose that our results incorporate the $\mathcal{O}(p^4)$ CHPT self-energies and resum higher order contributions, the following equations arise,

$$M_P^2 = \overset{\circ}{M}{}_P^2 + \Sigma_P^{4\chi}(\overset{\circ}{M}{}_Q^2; L_i^r) + \Sigma_P^H(\overset{\circ}{M}{}_Q^2; M_Q^2) \ . \tag{2.35}$$

Our analysis is performed in the isospin limit, $m_u = m_d = \hat{m}$ and no electromagnetic contributions. The symbols M_P^2 above refer to the masses of the lightest pseudoscalars in the isospin limit. To determine these masses we employ the Dashen theorem [64] which states that at the lowest nontrivial order in e^2 the neutral particles π^0 and K^0 do not receive electromagnetic contributions, while these are the same for $M^2_{\pi^+}$ and $M^2_{K^+}$. In this way,

$$M_\pi^2 = M_{\pi^0}^2 \simeq (135 \text{ MeV})^2 \ , \ M_K^2 = (M_{K^+} + M^2_{K^0} - M^2_{\pi^+} + M^2_{\pi^0})/2 \simeq (495 \text{ MeV})^2 \ , \tag{2.36}$$

are taken as the pion and kaon masses in the isospin limit, respectively. Violations of the previous relation for the pion mass are expected to be tiny, $\mathcal{O}((m_u - m_d)^2)$ [3], from the pure QCD side, and $\mathcal{O}(e^2 m_\pi^2/(8\pi^2 f_\pi^2))$ from electromagnetic interactions for the π^0 mass. More substantial seems to be the violations of the Dashen theorem for the kaon masses, of order $e^2 M_K^2$ [65, 66, 67]. So that, if we write $M_K^2 = \left[M^2_{K^+} + M^2_{K^0} - (1+\delta D)(M^2_{\pi^+} - M^2_{\pi^0})\right]/2$, with δD measuring the deviation with respect to the Dashen theorem, then as a conservative estimate, δD is expected to be in the range $0-2$ [30] from refs.[66, 67]. But even so, the changes in M_K^2 are at most a 0.5%, which can be discarded within the definitely larger uncertainties of our calculations, to be shown in the next sections.

3 Dynamical self-energies

We restrict in this section to eq.(2.34) and solve for $\overset{\circ}{M}{}^2_{\pi,K}$ (equivalently, for $B_0\hat{m}$ and $B_0 m_s$) and for M_η^2. In this section the η is actually the η_8 since we are not including any source of $\eta-\eta'$ mixing. The distinction between the η and η_8 is accomplished in the next section.

In perturbative studies one solves iteratively eq.(2.34). In this way, for the first round, we will use physical masses in all the arguments of the self-energies $\Sigma_P(\overset{\circ}{M}{}^2_Q; M_Q^2)$ with the resulting values

$$\overset{\circ}{M}_\pi = 108 \pm 4 \ , \ \overset{\circ}{M}_K = 422 \pm 18 \ , \ M_{\eta_8} = 660 \pm 17 \text{ MeV}. \tag{3.37}$$

The errors are calculated by performing a Monte-Carlo sampling of the free parameters of the T-matrix of ref.[20][#4] and varying the renormalization scale μ introduced above in the range between 0.5 and 1.2 GeV. This will be the standard procedure to evaluate errors in our work and should be understood in the following. Performing one more iteration in eq.(2.34), i.e. using the previous bare masses in the appropriate arguments of the self-energies, it results

$$\overset{\circ}{M}_\pi = 158 \pm 7 \ , \ \overset{\circ}{M}_K = 511 \pm 12 \ , \ M_{\eta_8} = 627 \pm 15 \text{ MeV}. \tag{3.38}$$

We observe significant differences between eqs.(3.37) and (3.38) for $\overset{\circ}{M}_\pi$ and $\overset{\circ}{M}_K$, which is a clear indication that higher orders corrections, of $\mathcal{O}(p^6)$ and superior, are relevant for the calculation of the lightest pseudoscalar self-energies in SU(3). This was also observed in refs.[7, 8], where the masses were calculated at $\mathcal{O}(p^6)$ in CHPT.

Because of the large variation between the values in eqs.(3.37) and (3.38), eq.(2.34) should be solved exactly. This is done by minimizing the function,

$$\begin{aligned} S(\overset{\circ}{M}_\pi, \overset{\circ}{M}_K) &= \left(\frac{\overset{\circ}{M}{}^2_\pi + \Sigma_\pi(\overset{\circ}{M}{}^2_Q; M_Q^2)}{M_\pi^2} - 1\right)^2 + \left(\frac{\overset{\circ}{M}{}^2_K + \Sigma_K(\overset{\circ}{M}{}^2_Q; M_Q^2)}{M_K^2} - 1\right)^2 \\ &+ \left(\frac{\overset{\circ}{M}{}^2_\eta + \Sigma_\eta(\overset{\circ}{M}{}^2_Q; M_Q^2) - M^2_{\eta_8}}{M_K^2}\right)^2 . \end{aligned} \tag{3.39}$$

[#4] We have made a new fit, including some more recent data, and the resulting fit has central values for the free parameters that are compatible with those of ref.[20], within the shown errors in this reference.

This method is more robust than the iterative one and it can provide solutions even when the later does not converge. On the other hand, since we are now varying the bare masses employed in the kernels for the T-matrices, we refit the scattering data in fig.1 for every value of the given bare masses. Then, the T-matrix changes as a function of the values employed in each step. The following results are obtained,

$$\overset{\circ}{M}_\pi = 126 \pm 4 \ , \ \ \overset{\circ}{M}_K = 476 \pm 10 \ , \ \ M_{\eta_8} = 635 \pm 15 \text{ MeV}. \tag{3.40}$$

One observes significant variations between the exact result and the first and second iterated solutions, eq.(3.37) and (3.38), respectively. This point is usually overlooked in the literature [3, 8]. Regarding the sizes of the self-energies we obtain

$$\frac{\Sigma_P(\overset{\circ}{M}{}_Q^2; M_Q^2)}{M_P^2} = 0.11 \pm 0.06 \ , \ 0.08 \pm 0.04 \ , 0.26 \pm 0.06 \ , \tag{3.41}$$

for pions, kaons and etas, respectively. We then observe that the physical masses of the pseudoscalars are dominated by the bare masses and that the dynamical contributions because of their self-interactions (which include the exchanges of the scalar resonances σ, κ, $f_0(980)$ and $a_0(980)$, as well as of the scalar octet of resonances around 1.4 GeV) are small. They are however somewhat more significant for the η_8 ($\overset{\circ}{M}_\eta = 545$ MeV from the Gell-Mann-Okubo relation). We then favour the standard CHPT scenario, where the linear quark mass term is assumed to dominate the pseudoscalar masses, versus the generalized one [68]. The M_{η_8} that we obtain, around 635 MeV, is larger than the one of the η physical meson, 547.45 MeV, that is very close to the bare η mass calculated from Gell-Mann-Okubo. Our value for M_{η_8} is very similar to that of ref.[36], $M_{\eta_8} = 639$ MeV.

Next, we also show our results for the solution of eq.(2.34) using the parameters in the S-waves with their values determined by fitting experimental data employing always physical masses in the interaction kernel. That is, we do not refit them in terms of the bare masses, as done previously. The resulting numbers

$$\overset{\circ}{M}_\pi = 125 \pm 4 \ , \ \ \overset{\circ}{M}_K = 477 \pm 10 \ , \ \ M_{\eta_8} = 633 \pm 15 \text{ MeV}, \tag{3.42}$$

are very similar to those already determined. The process of refitting the free parameters in the S-waves by distinguishing between physical and bare masses, where it corresponds, just introduces minor corrections (compared with the errors quoted) and will not be further considered in what follows.

Taking into account the expression of the bare masses in terms of the quark ones, eq.(2.32), and the values in eq.(3.40),

$$r_m = \frac{m_s}{\hat{m}} = 2\frac{\overset{\circ}{M}{}_K^2}{\overset{\circ}{M}{}_\pi^2} - 1 = 27.1 \pm 2.5 \ . \tag{3.43}$$

This number, within errors, is in the bulk of other determinations, $r_m = 25.7 \pm 2.6$ from $\mathcal{O}(p^4)$ CHPT [3], or with the more refined one of ref.[69], $r_m = 24.4 \pm 1.5$, and also with lattice determinations [30], 27.4 ± 0.5. It is worth stressing that our results in this section are predictions without any new free parameter. They are a consequence of the strong T-matrices used.

4 Including $\mathcal{O}(p^4)$ CHPT self-energies

In this section we consider eq.(2.35), which reproduces the CHPT self-energies at $\mathcal{O}(p^4)$ and the higher order contributions are estimated by adding Σ_P^H. The $\eta - \eta'$ mixing is incorporated at $\mathcal{O}(p^4)$ by the

$\times 10^3$	[7]	[35]		[70]
L_4^r	0	$\simeq 0.2$	0.2 ± 0.3 [71]	-0.3 ± 0.5
L_5^r	0.93 ± 0.11	$-$	$-$	1.4 ± 0.5
L_6^r	0	$\lesssim 0$	0.4 ± 0.2 [72]	-0.2 ± 0.3
L_7	-0.31 ± 0.14	$-$	$-$	-0.4 ± 0.2
L_8^r	0.60 ± 0.18	$-$	$-$	0.9 ± 0.3
$2L_6^r - L_4^r$	0	$\simeq -0.2$	0.6 ± 0.5	-0.1 ± 0.8
$2L_8^r - L_5^r$	0.23 ± 0.38	$-$	$-$	0.4 ± 0.8
$3L_7 + L_8^r$	-0.33 ± 0.46	$-$	$-$	-0.3 ± 0.7

Table 1: Values for some $\mathcal{O}(p^4)$ χPT counterterms $L_i^r(M_\rho) \times 10^3$ at the renormalization scale of the ρ mass from the literature.

counterterm L_7 and M_η is fixed to its physical value [3]. Eq.(2.35) incorporates the combinations of the low energy constants $L_{(5,8)} \equiv 2L_8^r - L_5^r$, $L_{(4,6)} \equiv 2L_6^r - L_4^r$ and $L_{(7,8)} \equiv 3L_7 + L_8^r$, eqs.(2.30) and (2.31). In table 1 we show values for these $\mathcal{O}(p^4)$ LECs at the mass of ρ resonance, $\mu = 770$ MeV. We show in the second column the so-called main fit from the $\mathcal{O}(p^6)$ fits of ref.[7] and in the fifth one those values from the $\mathcal{O}(p^4)$ fits of ref.[70]. In the fit shown of ref.[7] the large N_c suppression of the chiral counterterms L_4^r and L_6^r is used to fix their values to 0, although the precise scale at which this occurs it is not known. The error bands in the values of L_4^r and L_6^r in ref.[70], fifth column, are intended to cover this uncertainty. In this reference the null value for these counterterms is taken at the renormalization scale of the η meson mass. Other fits in ref.[7] are also given where this condition is relaxed and the differences are well taken into account by the estimated errors. In the third column we also show the values for L_4^r and L_6^r from the simultaneous study in ref.[35] of $\pi\pi$, $K\pi$ scattering together with the scalar form factors, the masses and decay constants of the lightest pseudoscalars, and $K_{\ell 4}$ decays at $\mathcal{O}(p^6)$ in CHPT with three flavours. The resulting values for such counterterms are found to be small and compatible with zero, in agreement with the large N_c suppression. Note that these new values of ref.[35], with vanishing L_4^r and L_6^r counterterms, reinforce the results of the main fit of ref.[7], where this was assumed. In refs.[71, 72] chiral sum rules are used to fix the latter counterterms to larger values. These determinations, however, suffer of the generally poor (if any) convergence of the three flavour CHPT series [8, 7, 35], with sizable $\mathcal{O}(p^6)$ contributions. Because CHPT with three flavours is used *only* at $\mathcal{O}(p^4)$ the determination of those counterterms incorporates large $\mathcal{O}(p^6)$ contributions, which are buried in the numbers given. We shall comment more on this issue with a precise example below. It should be understood for the third column in table 1 that when the value for a given L_i^r is not shown in the table this is the same as the one in the second column.

We first consider the matching at $\mathcal{O}(p^4)$ of the self-energies given in eqs.(2.34) and (2.35). The π and K self-energies given by eq.(2.34) at $\mathcal{O}(p^4)$ are

$$
\begin{aligned}
M_\pi^2 &= \mathring{M}_\pi^2 \left\{ 1 + \frac{\mathring{M}_\pi^2}{32\pi^2 f^2} \log \frac{\mathring{M}_\pi^2}{4\mu^2 e} - \frac{1}{3} \frac{\mathring{M}_\eta^2}{32\pi^2 f^2} \log \frac{\mathring{M}_\eta^2}{4\mu^2 e} \right\} , \\
M_K^2 &= \mathring{M}_K^2 \left\{ 1 + \frac{\mathring{M}_\eta^2}{48\pi^2 f^2} \log \frac{\mathring{M}_\eta^2}{4\mu^2 f^2} \right\} , \qquad (4.44)
\end{aligned}
$$

with $\log e = 1$. Comparing this expression with the one in eq.(2.30) one easily concludes that

$$L_{(4,6)}(\bar{\mu}) = -\frac{1}{36}\frac{1}{32\pi^2}\log\frac{\bar{\mu}^2}{4\mu^2 e} \quad , \quad L_{(5,8)}(\mu) = \frac{1}{6}\frac{1}{32\pi^2}\log\frac{\bar{\mu}^2}{4\mu^2 e} \ , \tag{4.45}$$

where $\bar{\mu}$ is the renormalization scale in CHPT and μ was already introduced in eq.(2.16). Notice that the expressions in eq.(4.45) are $\mathcal{O}(N_c^0)$, subleading in large N_c. This is certainly expected because this contribution originates from the loops resummed in eq.(2.34). Note that L_4^r and L_6^r are $\mathcal{O}(N_c^0)$, subleading in the large N_c counting, while L_5^r and L_8^r, separately, are of leading order, $\mathcal{O}(N_c)$. However, the combination $2L_8^r - L_5^r$ is numerically suppressed, as it is clear from the second column in table 1 from ref.[7]. In ref.[46] one gets the constraint $2L_8^r - L_5^r = 0$ by requiring that the strange scalar form factors vanish in the large N_c limit for $s \to \infty$.

From eq.(4.45) it follows that

$$L_{(5,8)} + 6L_{(4,6)} = 0 \ . \tag{4.46}$$

This is a robust output from our main assumption, namely, the dominance of S-wave rescattering in the lightest pseudoscalar self-energies in analogy with the one already well tested for the scalar form factors. Note that this relation is independent of the renormalization scheme chosen in the calculation of our integrals, contrary to the independent values of $2L_8^r - L_5^r$ and $2L_6^r - L_4^r$ in eq.(4.45). E.g. in these equations one has the appearance of the number e in the denominators of the logarithms as a remnant of our choice. This is removed in eq.(4.46), which is also independent of the renormalization scale $\bar{\mu}$ in CHPT.

One can also extract interesting consequences from eq.(4.46). Because of the factor six in front of $L_{(4,6)}$ and since $L_{(5,8)}$ is small in modulus,

$$L_{(4,6)} \simeq 0 \ . \tag{4.47}$$

This also implies that

$$L_6^r \simeq \frac{1}{2}L_4^r \ , \tag{4.48}$$

in good agreement with their most recent estimates in ref.[35] from $\mathcal{O}(p^6)$ CHPT, third column in table 1. As commented above, the values for L_4^r and L_6^r from refs.[71, 72] can suffer from large uncertainties due to the large $\mathcal{O}(p^6)$ contributions, because only CHPT at $\mathcal{O}(p^4)$ was used. As a example, if we take the central values for the bare masses in eq.(3.40), and evaluate with eq.(2.30) $L_{(4,6)}$ and $L_{(5,8)}$,

$$L_{(4,6)} = 0.23 \cdot 10^{-3} \ , \ L_{(5,8)} = 0 \ . \tag{4.49}$$

These numbers clearly violate the constraint in eq.(4.46). One would obtain $L_{(5,8)} \simeq -1.3 \cdot 10^{-3}$ if the previous value for $L_{(4,6)}$ were used in eq.(4.46). This is a clear example that $\mathcal{O}(p^6)$ contributions, and possibly also higher order ones, are so important in the CHPT series that unless they are taken proper and explicitly into account, an estimation of the $\mathcal{O}(p^4)$ counterterms from phenomenology with only $\mathcal{O}(p^4)$ CHPT is severely biased by large higher order contributions buried in the values obtained.

Next, we apply eq.(2.35) to study the physical masses of π, K and η. As a function of $L_{(4,6)}$ and $L_{(5,8)}$, we solve first for the $\overset{\circ}{M}{}_\pi^2$ and $\overset{\circ}{M}{}_K^2$ bare masses in eq.(2.35), and fix $\overset{\circ}{M}{}_\eta^2$ by the Gell-Mann-Okubo relation, eq.(2.33). $L_{(7,8)}$ is solved from the equation,

$$M_\eta^2 = \overset{\circ}{M}{}_\eta^2 + \Sigma_\eta^{4\chi}(\overset{\circ}{M}{}_Q^2) + \Sigma_\eta^H(\overset{\circ}{M}{}_Q^2; M_Q^2) \ , \tag{4.50}$$

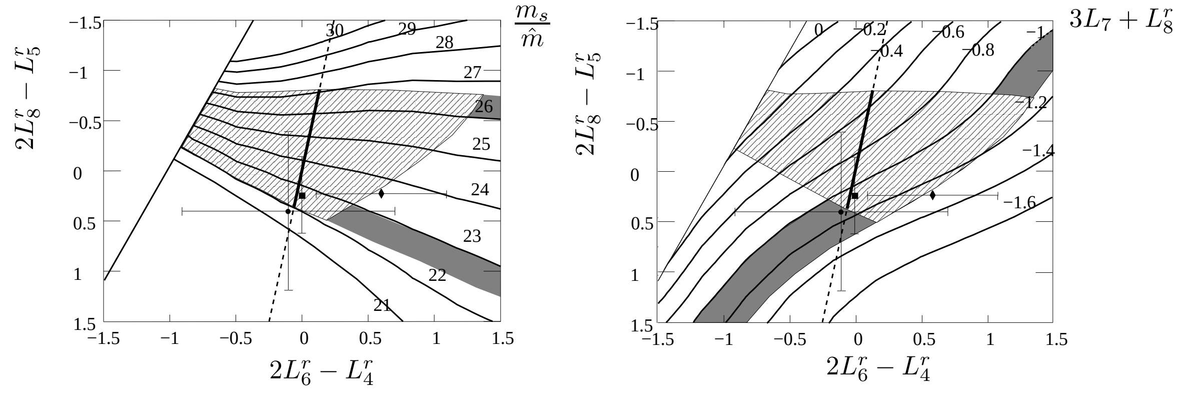

a)

b)

Figure 6: Left panel: Contour-plot for $r_m = m_s/\hat{m}$ as a function of $L_{(4,6)}$ and $L_{(5,8)}$. The square corresponds to the second column of table 1, the diamond to the fourth one and the circle to the fifth column. The straight line corresponds to the relation in eq.(4.46). No values for L_5^r nor L_8^r are provided in refs.[71, 72], and the absence of the vertical errorbar in the diamond refers to the fact that $L_{(5,8)}$ cannot be determined then from these references. Right panel: Contour-plot for $L_{(7,8)}$ as a function of $L_{(4,6)}$ and $L_{(5,8)}$. The meaning of the points is the same as in the left panel. Our results correspond to the values lying along the straight line within the stripped region, indicated by the thick solid line. For more details see the text.

We use the method of eq.(3.39) for solving eq.(2.35), though the last term on the r.h.s. of eq.(3.39) is removed since we are considering now the solution for $\overset{\circ}{M}_\pi$ and $\overset{\circ}{M}_K$. In fig.6a we show by the contour lines the calculated values for $r_m = m_s/\hat{m}$ as a function of $L_{(4,6)}$ and $L_{(5,8)}$ in units of 10^{-3}.[#5] The up-left corner where no contour lines are plotted determines a region where no solutions are found. The range of values for $L_{(4,6)}$ and $L_{(5,8)}$ has been chosen to span generously the values of table 1 within errors. If one takes into account that $m_s/\hat{m} = 24.4 \pm 1.5$ [69], the preferred region for $L_{(4,6)}$ and $L_{(5,8)}$ would be between the 23 and 26 contour lines. The shadowed areas below and above these lines, moving close to the 22 and 27 contour lines, represent the uncertainties of our calculations along them due to the variation in the renormalization scale, $\mu \sim [0.5, 1.2]$ GeV, and in the input parameters for the S-waves. In the figure, the square represents the values of $L_{(4,6)}$ and $L_{(5,8)}$ from ref.[7], second column in table 1. The full circle corresponds to the values in the last column of the same table and the diamond the value of $L_{(4,6)}$ in the fourth column, refs.[71, 72]. Notice that no values for L_5^r and L_8^r are provided in these references and hence no value for $L_{(5,8)}$ can be either determined. This is reflected in the absence of the vertical errorbar for the diamond. In the figure it is also shown the line corresponding to the constraint of eq.(4.46). We show in fig.6b a contour plot for the values of $L_{(7,8)}$ that are obtained from eq.(4.50). If one considers the values $L_{(7,8)} = -0.33 \pm 0.46$ [7] at $\mathcal{O}(p^6)$, and $L_{(7,8)} = -0.3 \pm 0.7$ [70] at $\mathcal{O}(p^4)$, the preferred $L_{(5,8)}$, $L_{(4,6)}$ region would be in the interval $\sim [-1, 0.4]$. Again the shadowed area along these lines represents the uncertainties of our calculation. The same points as in fig.6a are shown here and also the relation of eq.(4.46) is depicted by the straight line. The stripped area in the two figures represents the overlap between the favoured regions on them. Our values lie along the thick solid line defined by the intersection of the relation in the eq.(4.46) with the stripped region. It is certainly remarkable the large overlapping between this line and the square point from ref.[7]. Note that our approach and that of ref.[7] are completely independent. While refs.[35, 7] employ resonance saturation hypothesis to estimate the $\mathcal{O}(p^6)$ counterterms, which has an important impact on their NNLO results, we have made used of

---

[#5] In the whole manuscript, the values of the LECs displayed in the figures are given in units of 10^{-3} and referred to a renormalization scale equal to the ρ mass.

the dominant role of rescattering in meson-meson $I = 0$, $1/2$ and 1 scalar dynamics to calculate Σ_P^H. In addition, while refs.[35, 7] consider simultaneously the lightest pseudoscalar masses and decay constants, $K_{\ell 4}$ decays, scalar form factors and low energy $\pi\pi$, $K\pi$ scattering, we have considered all the scattering channels in the fig.1 and the π, K and η masses. Taking the intersection of the thick line in fig.6a and the square from ref.[7] at the one σ level, we end with the preferred interval of values

$$-0.15 \lesssim L_{(5,8)} \cdot 10^3 \lesssim 0.35 \;, \tag{4.51}$$

for $\bar{\mu} = M_\rho$. Let us recall also our previous estimate for $L_{(4,6)} \simeq 0$ in eq.(4.47).

We end this section with a remark. One can also use eq.(4.45) to derive values independently for $L_{(5,8)}$ and $L_{(4,6)}$. Nevertheless, these values are affected by the choice of the renormalization scheme, so that they can differ from those in the standard modified $\overline{MS}$ scheme of CHPT. In addition, allowing μ to change within the range $0.5 - 1.2$ GeV the range of values of $L_{(5,8)}$ is rather large and does not add any real new restriction to what it is already shown in fig.6. Notice that when we consider eq.(2.35) the $\mathcal{O}(p^4)$ contribution is given by $\Sigma_P^{4\chi}$, so that the L_i^r are considered properly in the same renormalization scheme as in CHPT. The same can be said for the relation in eq.(4.46) as it is invariant under any new constants that could be added when removing the infinite part to calculate the integral in eq.(2.17).

5 Comparison with lattice QCD results

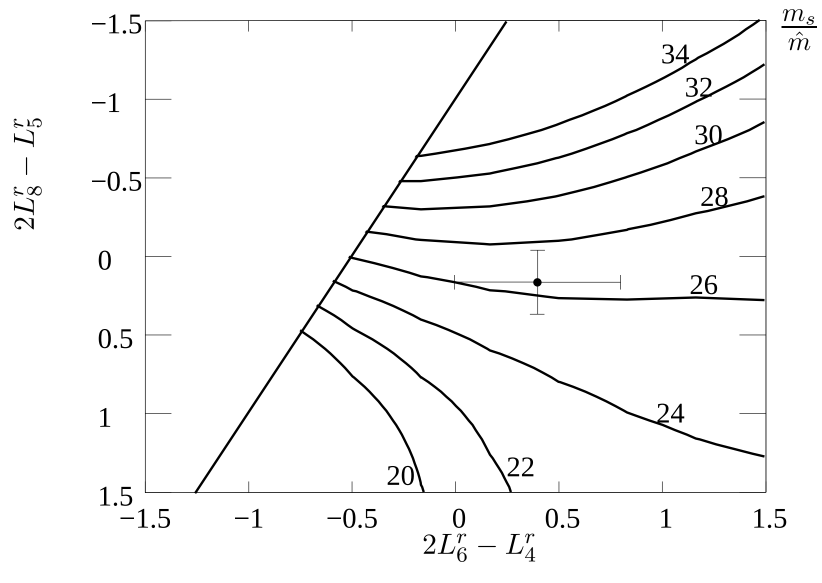

Figure 7: Contour-plot for $r_m = m_s/\hat{m}$ as a function of $L_{(4,6)}$ and $L_{(5,8)}$ obtained by employing only the $\mathcal{O}(p^4)$ CHPT self-energies. The point corresponds to the values of $L_{(5,8)}$ and $L_{(4,6)}$ from the MILC collaboration [31].

It is worth comparing the result in fig.6a with the calculation obtained by considering the self-energies only up to $\mathcal{O}(p^4)$ in CHPT, shown in fig.7. The difference in $m_s/\hat{m}$ for the same $L_{(4,6)}$ and $L_{(5,8)}$ is typically around $1 - 3$ units between both calculations, with larger values when only the $\mathcal{O}(p^4)$ CHPT self-energies are taken into account. A similar trend was also observed in ref.[8] from pure CHPT to $\mathcal{O}(p^6)$, with smaller values as higher orders in the chiral series are included. To $\mathcal{O}(p^4)$ the values 24.9 and 24.4 for r_m become, respectively, 24.1 and 23.3 to $\mathcal{O}(p^6)$ [8].

Two loop diagrams contributing to the self-energies were found very relevant numerically in ref.[8], larger by several factors than the $\mathcal{O}(p^4)$ contributions, similarly to what we find. Since diagrams with more than one loop were neglected in refs.[31, 30], worries arise about systematic uncertainties hidden in the values determined in these references for low energy parameters. To illustrate this point, we show in fig.7 by the solid circle the values $L_{(5,8)} = (0.16 \pm 0.20) \cdot 10^{-3}$ and $L_{(4,6)} = (0.4 \pm 0.4) \cdot 10^{-3}$ given by the QCD lattice calculation of the MILC Collaboration [31]. The latter reference also predicts $m_s/\hat{m} = 27.4 \pm 0.4$. It is worth stressing that this value is very close to the one obtained by considering only $\mathcal{O}(p^4)$ CHPT, as shown in the figure. Note that $\mathcal{O}(p^4)$ CHPT also includes at most diagrams with one chiral loop. As a result, we find quite reasonable to expect a reduction in the value of $m_s/\hat{m}$ of one unit at least, if higher loop diagrams were included, as we have done. Certainly, further arguments to those given in ref.[31] are necessary to rule out this expectation.

The MILC Collaboration also provides results for the pseudoscalar meson masses. We present next a good fit to these lattice data on the pseudoscalar masses (π and K), at the level of 1%, making use of eq.(2.35) for the self-energies. We are aware that our parameterization does not take into account the taste symmetry violating effects, due to the finite lattice spacing. Nevertheless, we think that our fit is valuable since the differences between our full results and those from a fit to lattice data with only $\mathcal{O}(p^4)$ CHPT, eq.(2.30), is an estimate of these diagrams with a higher number of loops. It provides then a rough quantification of systematic uncertainties that could affect the values for $L_{(4,6)}$, $L_{(5,8)}$ and $m_s/\hat{m}$ from refs.[30, 31, 32]. It is true that these references include $\mathcal{O}(p^6)$ contributions at tree level through the appropriate chiral counterterms in Staggered CHPT. Nevertheless, since two-loop diagrams, as well as one loop diagrams with higher order vertices, are neglected, the procedure is not systematic and some quantification is of interest.

We employ our eq.(2.35) to reproduce the quark mass dependence of the pseudoscalar masses provided by the MILC Collaboration [31] with three dynamical quarks and equal valence and sea quark masses. The systematic procedure to extrapolate these lattice results to the lightest quark masses in the continuum is to employing Staggered CHPT [33, 34] with three flavours. Nevertheless, present applications suffer of a huge proliferation of free parameters and include only diagrams involving at most one loop, though supplied with tree diagrams up to NNLO [31].

The strategy is the following. The MILC Collaboration [31] provides pseudoscalar meson masses as a function of the bare quark masses used. The current quark masses and the bare ones are proportional [30],

$$\overset{\circ}{M}{}^2_\pi = 2B_0 C(a) a\hat{m} \ , \quad \overset{\circ}{M}{}^2_K = B_0 C(a) a(\hat{m} + m_s) \ , \quad \overset{\circ}{M}{}^2_\eta = \frac{2}{3} B_0 C(a) a(\hat{m} + 2m_s) \ . \tag{5.52}$$

The dependence of the constant $C(a)$ with the lattice spacing can be found in ref.[32] at the two loop level, and in ref.[30] calculated up to the one loop order. Previous calculations with $C(a)$ at the one loop level [30] gave a value for $m_s^{\overline{MS}}(2\text{GeV}) = 76 \pm 8$ MeV, to be compared with the latest value given in ref.[32] $m_s^{\overline{MS}}(2\text{GeV}) = 87 \pm 6$ MeV. This substantial shift upwards comes from the improvement in the determination of $C(a)$ by moving from the one to the two loop calculation. We use in our fits the two loop result for $C(a)$ from ref.[32]. Ref.[31] gives the so called “coarse” lattice runs with $a_{coarse} \simeq 0.12$ fm, and the “fine” lattices with $a_{fine} \simeq 0.09$ fm, with an error in a about 1.2%. Making use of ref.[32] we then determine that $C(a_{fine})/C(a_{coarse}) = 2.76/1.85 = 1.49$ for $\mu = 2$ GeV. From this relation we fix $C(a_{fine})$ in terms of $C(a_{coarse})$ and take the latter as a free parameter, denoted in the following just as C. As the constant C does not depend on the value of the quark mass in very good numerical accuracy (at the level of 0.1% [30, 32]), we then employ the same value for all the quark masses used in the lattice runs with the same a. We solve eq.(2.35) for the kaon and pion masses given by lattice QCD in terms of the bare quark masses used. From the mass equations at the physical point one can obtain $L_{(4,6)}$ and $L_{(5,8)}$

as a function of $\overset{\circ}{M}{}^2_\pi$ and $\overset{\circ}{M}{}^2_K$. Hence, the only free parameters in the fit to lattice data are B_0C, $\overset{\circ}{M}{}^2_\pi$ and $\overset{\circ}{M}{}^2_K$. In the fit we do not consider the two points of the fine lattice run with $m_s/\hat{m} = 0.031/0.0124 = 2.5$, because it implies a rather heavy pion with a mass of 470 MeV [31]. We then restrict ourselves to the case of lighter pions with $m_s/\hat{m} \geq 5$. In figs.8a, b, we show the reproduction of the lattice points [31] and of the physical values for the pion and kaon masses, respectively. The size of the squares corresponds to a relative error of 1.2%, the one given to a [31]. The circles correspond to our points for the coarse lattices, the triangles for the fine ones and the arrows indicate the values of the physical kaon and pion masses. It is also worth stressing that the scattering data in fig.1 are simultaneously reproduced.[#6] From this fit we get the values,

$$2L_8^r - L_5^r = -0.52 \pm 0.43 \quad , \quad 2L_6^r - L_4^r = -0.20 \pm 0.17 \ . \tag{5.53}$$

In fig.9 we show by the solid ellipse the one sigma region for $L_{(4,6)}$ and $L_{(5,8)}$ obtained in our fit, from where one can infer the correlation between these two parameters. We also show the straight line from eq.(4.46), the square point corresponding to ref.[7], second column in table 1, and by the circle we show the values

$$2L_8^r - L_5^r = 0.16 \pm 0.20 \quad , \quad 2L_6^r - L_4^r = 0.4 \pm 0.4 \ , \tag{5.54}$$

obtained by the MILC Collaboration [30, 31]. The fact that the values in eq.(5.53) do not lie within the favoured region in fig.9 is an indication of non-negligible finite lattice spacing effects, already stressed in ref.[31]. The MILC values in eq.(5.54) are barely compatible, at the level of one sigma, with the thick solid line shown inside the stripped region and with the square from ref.[7].

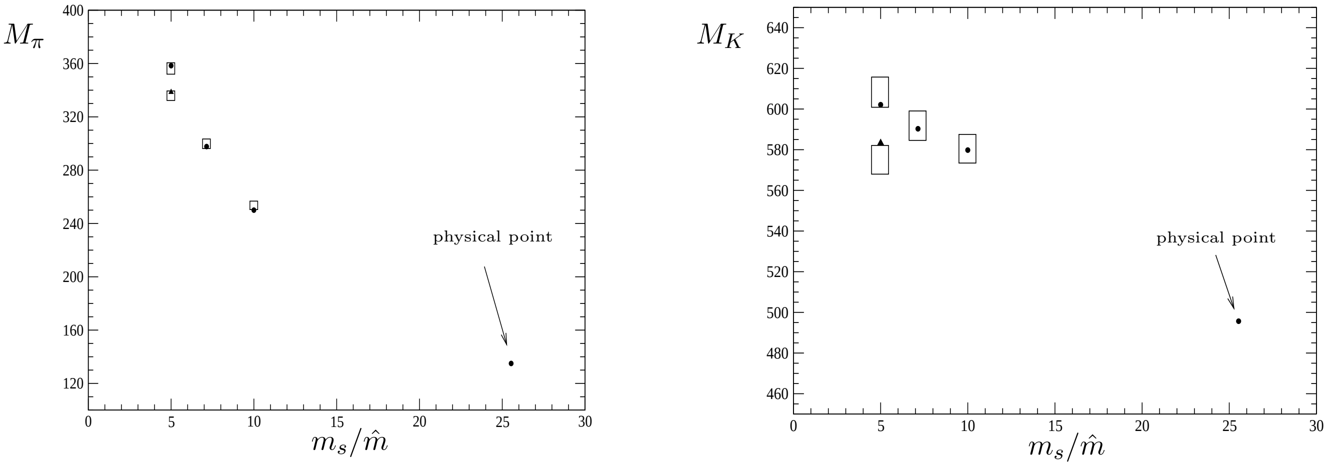

Figure 8: Lattice data from the MILC Collaboration [31] and their reproduction by our parameterization. The masses are given in MeV. The size of the squares corresponds to a relative error of 1.2%, the one given to a in ref.[31]. The circles refer to our calculations for the coarse lattices and the triangles for the fine ones. The physical mass values are signalled out by an arrow.

We have also performed a fit employing only the self-energies calculated at $\mathcal{O}(p^4)$ in CHPT. The result obtained from the fit to the lattice data is $2L_8^r - L_5^r = -0.20 \cdot 10^{-3}$ and $2L_6^r - L_4^r = 0.13 \cdot 10^{-3}$

[#6] In the fit to the unphysical points of lattice the dependence on the bare masses of the pseudoscalar decay constants f_π, f_K and f_η, generally called f_P, could play a role. We have then also performed fits to the lattice data recalculating the f_P in terms of the $\mathcal{O}(p^4)$ CHPT expressions for f_P as a function of the bare masses, with values for L_4^r and L_5^r such that at the physical point the constants f_P have their physical values. As we have checked, these considerations affect little the resulting fit and the results are well within the uncertainty bounds quoted before.

and these data is quite well reproduced. The difference with respect to eq.(5.53) is due to the extra unitarity loops and higher order effects from the exchanges of tree level resonances. The former effects are not systematically considered in ref.[31]. The size of this difference is then an estimate of systematic uncertainties that could affect those results from ref.[31] and that, when added in quadrature with the errors given, would enlarge by a factor ∼ 2 the errorbar for $L_{(5,8)}$ in eq.(5.54).

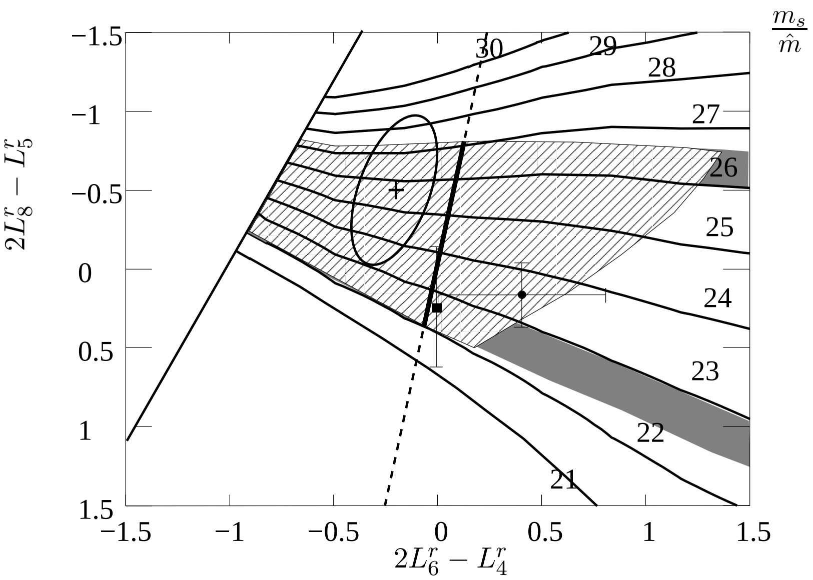

Figure 9: Contour-plot for $r_m = m_s/\hat{m}$ as a function of $L_{(4,6)}$ and $L_{(5,8)}$, showing also the ellipse of the fitted values in eq.(5.53). The circle corresponds to the lattice extrapolation from Staggered CHPT [31]. The rest is the same as in fig.6a.

From the favoured region in fig.6a, given by the intersection of the straight line with the stripped region and the square point within errorbars, it results

$$\frac{m_s}{\hat{m}} = 22 - 25 \ . \tag{5.55}$$

This value is in good agreement with 24.4 ± 1.5 from ref.[69]. The previous result is somewhat lower than the value 27.4 ± 0.5 from the MILC Collaboration [30] and ref.[32]. As discussed above, we consider that this difference is mostly due to the non inclusion of higher loop diagrams in the Staggered CHPT extrapolations used in these references. It follows from this discussion that those calculations are necessary to settle this issue. Within the same favoured region of values for $L_{(4,6)}$ and $L_{(6,8)}$ we also obtain,

$$L_{(7,8)} = -(0.7 - 1.1) \cdot 10^{-3} \ , \tag{5.56}$$

and

$$\overset{\circ}{M}_\pi = 116 - 119 \ , \ \ \overset{\circ}{M}_K = 400 - 420 \ \text{ MeV}. \tag{5.57}$$

Finally, we give in table 2 the relative sizes of $\Sigma_P^{4\chi}$ and Σ_P^H for the same interval of values for $L_{(5,8)}$, eq.(4.51), and $L_{(4,6)} = 0$. The fact that Σ_P^H is larger than $\Sigma_P^{4\chi}$ is in agreement with ref.[7]. Indeed, the sizes of our self-energies from Σ_P^H are rather similar to those determined in this reference to $\mathcal{O}(p^6)$. Ref.[8] obtains: $\Sigma_\pi^{6\chi}/M_\pi^2 = 0.132 - 0.355$, $\Sigma_K^{6\chi}/M_K^2 = 0.194 - 0.423$ and $\Sigma_\eta^{6\chi}/M_\eta^2 = 0.234 - 0.521$. These values are well inside our bulk of results in table 2. Thus, the calculations of ref.[7] to $\mathcal{O}(p^6)$, although showing

	π	K	η
$\Sigma_P^{4\chi}/M_P^2$	$[-0.010, 0.015]$	$[-0.01, -0.07]$	$[-0.16, -0.18]$
Σ_P^{H}/M_P^2	$[0.233, 0.235]$	$[0.352, 0.358]$	$[0.445, 0.460]$
$\Sigma_P^{4\chi}/\Sigma_P^{H}$	$[-0.05, 0.06]$	$[-0.03, -0.20]$	$[-0.37, -0.40]$

Table 2: Relative sizes of the $\mathcal{O}(p^4)$, $\mathcal{O}(p^6)$ and higher order contributions to the self-energies. The intervals corresponds to the interval of values for $L_{(5,8)}$ in eq.(4.51) and $L_{(4,6)} = 0$.

that this order is much larger than the $\mathcal{O}(p^4)$, does not imply necessarily the lack of convergence of the chiral series. Our calculation, estimating higher orders corrections by incorporating physical S-waves which include both resonant and non-resonant dynamics, gives us values of similar size to those of this reference up to $\mathcal{O}(p^6)$. In addition, we have to recall the agreement between the straight line in fig.6a, determined from an algebraic matching at $\mathcal{O}(p^4)$ of eqs.(2.34) and (2.35), and the square from ref.[7], determined numerically from a phenomenological analysis to $\mathcal{O}(p^6)$.

6 Conclusions

We have undertaken a non-perturbative chiral study of the self-energies of the lightest pseudoscalar mesons. In their evaluation the S-wave amplitudes obtained in UCHPT, that reproduce scattering data very accurately up to around 1.4 GeV, are employed. These amplitudes generate the exchange of the nonet of the lightest scalar resonances, σ, $f_0(980)$, $a_0(980)$ and κ, whose contributions to the pseudoscalar masses are expected to be relevant since they significantly affect the scalar form factors [26, 29, 73, 74]. The latter are tightly related to the pseudoscalar self-energies due to the Feynman-Hellman theorem. As stressed, their contributions have to be calculated simultaneously with those from the unitarity loops, since these resonances due their origin to the large unitarity contributions driven by chiral symmetry.

We determine that the pseudoscalar masses squared for π and K are dominated by the bare ones, with the self-energy contributions not larger than 10%. For the η meson they can be larger but still lower than around 30%. This favors standard CHPT versus its generalized scenario. We also determine the mass of the η_8, $M_{\eta_8} = 635$ MeV, in agreement with a previous determination. Next, we take the exact $\mathcal{O}(p^4)$ CHPT self-energies and resum the higher order contributions within our approach. Matching algebraically at $\mathcal{O}(p^4)$ with the calculated self-energies from CHPT one obtains the relation $L_{(5,8)} = -6L_{(4,6)}$, which is independent of the renormalization scale and of our choice of renormalization scheme. From this relation it follows that $L_{(4,6)} \simeq 0$ and thus $L_6^r \simeq L_4^r/2$, in good agreement with the $\mathcal{O}(p^6)$ CHPT results from ref.[7]. Considering as well the value of the quark mass ratio $m_s/\hat{m} = 24.4 \pm 1.5$ from ref.[69], and the values for $L_{(7,8)}$ from refs.[7, 70], we delimit a shorter interval of values for $L_{(5,8)}$ lying along the line $L_{(5,8)} + 6L_{(4,6)} = 0$. The value obtained from refs.[35, 7] perfectly overlaps with our determination, and the common intersection between these two independents methods gives $-0.15 \lesssim L_{(5,8)} \cdot 10^3 \lesssim 0.35$. This implies that we estimate $m_s/\hat{m} = 22 - 25$ and $L_{(7,8)} = -(0.7 - 1.1) \cdot 10^{-3}$. We also warn about higher loop diagram effects in the chiral series when evaluating $m_s/\hat{m}$, as they tend to decrease the value for this ratio. This is relevant for its recent calculation from lattice QCD [31] as these higher loop effects are not systematically accounted for in present extrapolations to physical light quark masses and the continuum. Their evaluation is called for. We have also offered a good reproduction of the lattice pseudoscalar masses, though the fitted values for $L_{(4,6)}$ and $L_{(5,8)}$ are outside the previous favoured region. This is considered as a clear indication of discretization effects not yet negligible in the lattice data, as already stressed in ref.[31].

Other interesting result from our investigation is that although the $\mathcal{O}(p^6)$ contribution to the self-energies calculated in three flavour CHPT [8] is much larger than the $\mathcal{O}(p^4)$ ones, we still obtain self-energies of similar values to those of ref.[8] despite higher order corrections are also included. This fact together with our agreement with ref.[7] in the values for $L_{(4,6)}$ and $L_{(5,8)}$, indicate that the SU(3) CHPT expansion is not spoiled once the $\mathcal{O}(p^6)$ is taken into account.

Acknowledgements

Financial support by MEC (Spain) grants No. FPA2004-62777, No. FPA2007-62777, No. BFM-2003-00856, Fundación Séneca (Murcia) grant Ref. 02975/PI/05, the European Commission (EC) RTN Program Network "EURIDICE" Contract No. HPRN-CT-2002-00311 and the HadronPhysics I3 Project (EC) Contract No. RII3-CT-2004-506078 is acknowledged.

References

[1] S. Weinberg, Physica **A96** (1979) 327.

[2] J. Gasser and H. Leutwyler, Ann. Phys. **158** (1984) 142.

[3] J. Gasser and H. Leutwyler, Nucl. Phys. **B250** (1985) 465.

[4] J. Bijnens, G. Colangelo and G. Ecker, JHEP **9902** (1999) 020.

[5] J. Bijnens, G. Colangelo and G. Ecker, Annals Phys. **280** (2000) 100.

[6] J. Bijnens, AIP Conf. Proc. **698** (2004) 407, and references therein.

[7] G. Amoros, J. Bijnens and P. Talavera, Nucl. Phys. **B585** (2000) 293; (E)-ibid. **B598** (2001) 665.

[8] G. Amoros, J. Bijnens and P. Talavera, Nucl. Phys. **B568** (2000) 319.

[9] B. Ananthanarayan, G. Colangelo, J. Gasser and H. Leutwyler, Phys. Rept. **353** (2001) 207; G. Colangelo, J. Gasser and H. Leutwyler, Phys. Lett. **B488** (2000) 261; I. Caprini, G. Colangelo, J. Gasser and H. Leutwyler, Phys. Rev. **D68** (2003) 074006.

[10] S. Descotes-Genon, N. H. Fuchs, L. Girlanda and J. Stern, Eur. Phys. J. **C24** (2002) 469.

[11] J. R. Pelaez and F. J. Yndurain, Phys. Rev. **D71** (2005) 074016; Phys. Rev. **D68** (2003) 074005; R. Kaminski, J. R. Pelaez and F. J. Yndurain, arXiv:hep-ph/0603170.

[12] J. Gasser and H. Leutwyler, Nucl. Phys. **B250** (1985) 539.

[13] C. Roiesnel and T. N. Truong, Nucl. Phys. **B187** (1981) 293; T. N. Truong, Phys. Rev. Lett. **61** (1988) 2526; Phys. Lett. **B207** (1988) 495.

[14] Bellucci, J. Gasser and M. E. Sainio, Nucl. Phys. **B423**, 80 (1994).

[15] J. Gasser, M. A. Ivanov and M. E. Sainio, Nucl. Phys. **B728**, 31 (2005).

[16] J. A. Oller, L. Roca and C. Schat, arXiv:0708.1659 [hep-ph], to appear in Physics Letters **B**.

[17] D. Morgan and M. R. Pennington, Z. Phys. **C37**, 431 (1988); (E)-ibid. **C39** (1988) 590; Phys. Lett. **B272** (1991) 134 .

[18] M. R. Pennington, pag.18 in L. Maiani, G. Panchieri and N. Paver, eds., The DAΦNE Physics Handbook (INFN, Frascati, 1992); Phys. Rev. Lett. **97** (2006) 011601.

[19] J. A. Oller and E. Oset, Nucl. Phys. **A620** (1997) 438; (E)-ibid. **A652** (1999) 407.

[20] J. A. Oller and E. Oset, Phys. Rev. **D60** (1999) 074023.

[21] M. Jamin, J. A. Oller and A. Pich, Nucl. Phys. **B587** (2000) 331

[22] A. Dobado and J. R. Pelaez, Phys. Rev. **D56** (1997) 3057.

[23] H. Hellman, "Einfürung in die Quantenchemie", Deuticke Verlag, Leipzig, 1937; R. P. Feynman, Phys. Rev. **56** (1939) 340; S. T. Epstein, Amer. J. Phys. **22** (1954) 613.

[24] J. Gasser, Ann. Phys. **136** (1981) 62.

[25] J. Gasser, H. Leutwyler and M. E. Sainio, Phys. Lett. B **253** (1991) 252; Phys. Lett. B **253** (1991) 260.

[26] J. Gasser and U.-G. Meißner, Nucl. Phys. **B357** (1991) 90.

[27] J. Gasser and H. Leutwyler, Nucl. Phys. **B250** (1985) 517.

[28] T. N. Truong, *"Unitarized chiral perturbation theory and rare decay of mesons.* Lectures given at Ettore Majoranava International School on Low Energy Antiproton Physics, Erice, Italy, Jan 25-31, 1990. Erice School Phys. (1990) 65.

[29] U. G. Meißner and J. A. Oller, Nucl. Phys. **A679** (2001) 671; T. A. Lahde and U. G. Meißner, Phys. Rev. **D74**, 034021 (2006).

[30] C. Aubin *et al.*, Phys. Rev. **D70** (2004) 031504.

[31] C. Aubin *et al.*, Phys. Rev. **D70** (2004) 094505; Phys. Rev. **D70** (2004) 114501.

[32] Q. Mason, H. D. Trottier, R. Horgan, C. T. H. Davies and G. P. Lepage [HPQCD Collaboration], Phys. Rev. **D73** (2006) 114501.

[33] W. J. Lee and S. R. Sharpe, Phys. Rev. **D60** (1999) 114503.

[34] C. Aubin and C. Bernard, Phys. Rev. **D68** (2003) 034014.

[35] J. Bijnens, P. Dhonte and P. Talavera, JHEP **0405** (2004) 036.

[36] G. Ecker, J. Gasser, A. Pich and E. de Rafael, Nucl. Phys. **B321** (1989) 311.

[37] J. A. Oller and U. G. Meißner, Phys. Lett. **B500** (2001) 263.

[38] J. A. Oller, Phys. Lett. **B477** (2000) 187.

[39] J. A. Oller, E. Oset and J. R. Pelaez, Phys. Rev. Lett. **80** (1998) 3452; Phys. Rev. **D59** (1999) 074001; (E)-ibid. **D60** (1999) 099906.

[40] J. A. Oller, Nucl. Phys. **A727** (2003) 353.

[41] I. Caprini, G. Colangelo and H. Leutwyler, Phys. Rev. Lett. **96** (2006) 132001.

[42] E. M. Aitala *et al.* [E791 Collaboration], Phys. Rev. Lett. **86** (2001) 770; Phys. Rev. Lett. **89** (2002) 121801.

[43] S. Descotes-Genon and B. Moussallam, Eur. Phys. J. **C48** (2006) 553.

[44] E. van Beveren *et al.*, Z. Phys. **C30** (1986) 615.

[45] W. M. Yao *et al.* [Particle Data Group], J. Phys. **G33** (2006) 1.

[46] M. Jamin, J. A. Oller and A. Pich, Nucl. Phys. **B622** (2002) 279.

[47] B. Hyams et al., Nucl. Phys. B 64 (1973) 134; P. Estrabooks et al., AIP Conf. Proc. 13 (1973) 37; G. Grayer et al., Proc. 3rd Philadelphia Conf. on Experimental Meson Spectroscopy, Philadelphia, 1972 (American Institute of Physics, New York, 1972) 5; S.D. Protopopescu and M. Alson-Garnjost, Phys. Rev. **D7** (1973) 1279.

[48] R. Kaminski, L. Lesniak and K. Rybicki, Z. Phys. **C74** (1997) 79.

[49] W. Ochs, University of Munich, thesis, 1974.

[50] C.D. Frogratt and J.L. Petersen, Nucl. Phys. **B129** (1977) 89.

[51] D. H. Cohen, D. S. Ayres, R. Diebold, S. L. Kramer, A. J. Pawlicki and A. B. Wicklund, Phys. Rev. **D22** (1980) 2595.

[52] A. Etkin et al., Phys. Rev. **D28** (1982) 1786.

[53] W. Wetzel et al., Nucl. Phys. **B115** (1976) 208; V.A. Polychronakos et al., Phys. Rev. **D19** (1979) 1317; G. Costa et al., Nucl. Phys. **B175** (1980) 402.

[54] R. Mercer et al., Nucl. Phys. **B32** (1971) 381.

[55] P. Estabrooks, R. K. Carnegie, A. D. Martin, W. M. Dunwoodie, T. A. Lasinski and D. W. G. Leith, Nucl. Phys. B **133**, 490 (1978).

[56] T.A. Armstrong et al., Z. Phys. **C52** (1991) 389.

[57] D. Linglin *et al.*, Nucl. Phys. **B57** (1973) 64.

[58] A. D. Martin and E. N. Ozmutlu, Nucl. Phys. **B158** (1979) 520.

[59] L. Rosselet et al., Phys. Rev. **D15** (1997) 574.

[60] J.A. Oller, Phys. Rev. **D71** (2005) 054030.

[61] V. Bernard, T. R. Hemmert and U. G. Meißner, Nucl. Phys. **A732** (2004) 149.

[62] E. Epelbaum, W. Gloeckle and U. G. Meißner, Eur. Phys. J. **A19** (2004) 125.

[63] J. F. Donoghue, B. R. Holstein and B. Borasoy, Phys. Rev. **D59** (1999) 036002.

[64] R. F. Dashen, Phys. Rev. **183** (1969) 1245.

[65] J. F. Donoghue, B. R. Holstein and D. Wyler, Phys. Rev. **D47** (1993) 2089.

[66] R. Urech, Nucl. Phys. **B433** (1995) 234.

[67] J. Bijnens and J. Prades, Nucl. Phys. **B490** (1997) 239.

[68] N. H. Fuchs, H. Sazdjian and J. Stern, Phys. Lett. **B269** (1991) 183; J. Stern, H. Sazdjian and N. H. Fuchs, Phys. Rev. **D47** (1993) 3814.

[69] H. Leutwyler, Phys. Lett. **B378** (1996) 313.

[70] J. Bijnens, G. Colangelo and J. Gasser, Nucl. Phys. **B427** (1994) 427.

[71] B. Ananthanarayan, P. Buettiker and B. Moussallam, Eur. Phys. J. **C22** (2001) 133.

[72] B. Moussallam, Eur. Phys. J. **C14** (2000) 111.

[73] J. A. Oller and L. Roca, Phys. Lett. B **651** (2007) 139.

[74] F. J. Ynduráin, Phys. Lett. **B612** (2005) 245; Phys. Lett. **B578** (2004) 99; (E)-*ibid.* **B586** (2004) 439.